ISSN 0869-5911, Petrology, 2006, Vol. 14, No. 5, pp. 452–476. © Pleiades Publishing, Inc., 2006.
Original Russian Text © V.I. Kovalenko, V.B. Naumov, A.V. Girnis, V.A. Dorofeeva, V.V. Yarmolyuk, 2006, published in Petrologiya, 2006, Vol. 14, No. 5, pp. 482–507.

# Composition and Chemical Structure of Oceanic Mantle Plumes

**V. I. Kovalenko[a], V. B. Naumov[b], A. V. Girnis[a], V. A. Dorofeeva[b], and V. V. Yarmolyuk[a]**

[a] *Institute of Geology of Ore Deposits, Petrography, Mineralogy, and Geochemistry (IGEM), Russian Academy of Sciences, Staromonetnyi per. 35, Moscow, 109017 Russia*
*e-mail: vik@igem.ru*

[b] *Vernadsky Institute of Geochemistry and Analytical Chemistry, Russian Academy of Sciences, ul. Kosygina 19, Moscow, 119991 Russia*
*e-mail: naumov@geokhi.ru*

Received October 20, 2005

**Abstract**—The average compositions (including $H_2O$, Cl, F, and S contents) and chemical structure of oceanic mantle plumes were estimated on the basis of the ratios of incompatible volatile components, potassium, and some other elements in the basaltic magmas of ocean islands (melt inclusions and quenched glasses). The following average concentrations were estimated for the plume mantle: 510 ppm $K_2O$, 520 ppm $H_2O$, 21 ppm Cl, 55 ppm F, and 83 ppm S; these values are significantly higher than those of the depleted mantle (except for S). The abundances of $H_2O$, Cl, and S are lower than in the primitive mantle. The normalized $H_2O$ content in the plume mantle is similar to the concentrations of similarly incompatible La and Ce but lower than the concentrations of $K_2O$, Cl, and Sr. This is at odds with the idea of wet mantle plumes. Three types of basaltic magmas corresponding to three types of plume sources (M1, M2, and M3) were distinguished. The concentrations of incompatible elements in these reservoirs were estimated using two models, assuming either an isochemical mantle or a moderately enriched composition of plume material. The latter model gave the following average concentrations of $H_2O$, Cl, F, and S: 130, 33, 11, and 110 ppm for M1, 110, 12, 65, and 45 ppm for M2; 530, 29, 49, and 110 ppm for M3. The plume mantle is not homogeneous, and its heterogeneity is related to the existence of three main compositions, one of which (M1) is similar to the mantle of mid-ocean ridges, and two others (M2 and M3) are moderately enriched in $K_2O$, $TiO_2$, $P_2O_5$, F, and incompatible trace elements. The compositions of M2 and M3 are strongly different in $H_2O$, Cl, and S contents. The M2 mantle reservoir is significantly poorer in these components and richer in incompatible trace elements than M3. The plume mantle was formed mainly by the mixing of three sources: ultradepleted mantle, moderately enriched relatively dry mantle, and moderately enriched $H_2O$-rich mantle. In addition to the three main components of the plume mantle, there are probably minor components enriched in chlorine and depleted in fluorine. It is supposed that all these components are entrained into the plume mantle through the mantle recycling of components of the oceanic and continental crust. The established relationships are in agreement with the zonal model of a mantle plume, which includes a hot central part poor in $H_2O$, Cl, and S; an outer part enriched in volatile and nonvolatile incompatible elements; and enclosing mantle material interacting with the plume.

**DOI:** 10.1134/S0869591106050031

## PROBLEM FORMULATION AND FACTUAL BASIS

This paper addresses the problem of the composition of basic magma sources for ocean islands and plateaus in order to develop a generalized model for the chemical structure of mantle plumes. The factual basis includes 800 measurements of $H_2O$, about 1400 measurements of Cl, more than 800 of F, 3300 of K and Ti, 2900 of P, and some other chemical elements in melt inclusions and quench glasses compiled in our database (Naumov et al., 2000, 2004). The analytical data represent various oceanic islands, plateaus, and bottoms of adjoining basins. The literature sources are presented elsewhere (Kovalenko et al., 2006b). A number of models have been proposed for the formation of ocean island magmas and their sources in particular regions, but generalized models considering the main compositional features of such magmas are yet not adequately developed. One of the reasons is the absence of global compilations for the compositions of magmas in these environments, including reliable estimates of the average contents of volatile components. One of the goals of this study was to estimate the average compositions of ocean island magmas and determine on this basis the average contents of volatile components in the magma sources, i.e., in mantle plumes. Some aspects of this problem were considered in our previous publications (Kovalenko et al., 2006b, 2006c), and this paper presents its general solution.

## GENERAL APPROACH

In order to solve the problem, we assumed, first, that the compositions of melt inclusions and quenched glasses correspond to the compositions of natural mag-

mas. This is especially important for volatile components, which are not retained in crystalline igneous rocks. The possible effects of volatile (primarily, hydrogen) loss from inclusions (Quin et al., 1992; Sobolev and Danyushevsky, 1994; Massare et al., 2002; Hauri, 2002) were ignored. The difference between the average compositions of glasses of rocks and melt inclusions results mainly from the different degrees of their differentiation, whereas the influence of volatile loss after inclusion entrapment is on average negligible (Kovalenko et al., 2006a). Therefore, such a simplification is not only inevitable but also justified. Second, we assumed that the components $H_2O$, Cl, F, K, Ti, and P considered in this paper are incompatible in mantle materials, i.e., the bulk partition coefficients of these components between solid phases and melt are low. It was therefore assumed that the concentration ratios of water, chlorine, and fluorine with each other and to other incompatible elements (potassium, titanium, and phosphorus) in basic magmas are to a first approximation identical to the corresponding ratios in the sources of these magmas (Hofmann, 1997). It is desirable to use the ratios of components with similar bulk crystal–melt partition coefficients (Hofmann, 2003). Before analyzing the average composition and chemical variations in plume magmas, it is expedient to estimate the influence of the difference in the incompatibility of components on the difference in the proportions of these components in melts and their sources.

Element ratios in mantle melts depend on the conditions and mechanisms of magma extraction. The real mechanism of this process is probably close to critical melting, which is transitional between batch and fractional melting. Therefore, element ratios in melts obtained by batch and fractional melting can be considered as constraining possible variations in the natural process. The concentration of element **1** in melt ($C_1$) is a function of the degree of source rock melting ($F$), the bulk solid–liquid partition coefficient of the element ($D$), and the initial concentration of the element in the source ($C_1^0$) (Ryabchikov, 1965; Shaw, 1970):

$$C_1 = C_1^0/[D + F(1 - D)] \quad (1)$$

for batch melting and

$$C_1 = C_1^0 [1 - (1 - F)^{1/D}]/F \quad (2)$$

for fractional melting.

The difference between the ratios of elements **1** and **2** in a melt and its mantle source increases as $F$ approaches the maximum $D$ value (Maaloe, 1994). In order to quantify these effects, let us consider the concentration ratio $C_1/C_2$, where the partition coefficient for element **2** is taken to be very low ($D_2 = 10^{-5}$). Another important characteristic of the process of melt extraction is the amount of melt ($z$) retained in the mantle after the removal of the major portion of liquid. We

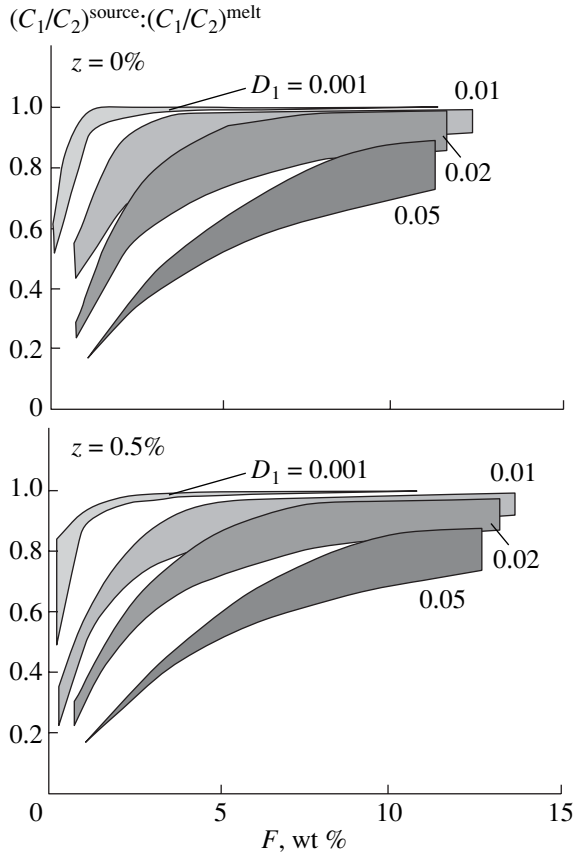


**Fig. 1.** Calculated variations in the concentration ratios of two incompatible elements in melt at low degrees of mantle source melting ($F$). $C_1$ and $C_2$ are the concentrations of elements **1** and **2**; the bulk partition coefficient of element **1** between solid and liquid phases ($D_1$) varies from 0.001 to 0.05, and element **2** has a very small $D_2$ value of $10^{-5}$. The range presented for each $D_1$ value corresponds to variations in the mechanisms of melt separation, from batch to fractional melting. The upper and lower panels were calculated for two different values of the fraction of partial melt retained in the crystal matrix after the separation of the main portion of liquid ($z$ = 0 and 0.5%, respectively).

calculated melt compositions for $z = 0$ and $z = 0.005$ (0.5%).

The results of calculations are presented in Fig. 1, which demonstrates that the $C_1/C_2$ ratio may be strongly different from the source (mantle) value at low degrees of melting and (or) high partition coefficient of more compatible element **1**. The ratio of elements **1** and **2** in a magma is identical to that of the source if $D_2 - D_1 = 0$ or the degree of melting is one (Hofmann, 1997). As can be seen from Fig. 1, up to $D_2 - D_1 = 0.03$ (K, Ce, $H_2O$, Cl, F, P, Ti, and many other trace elements), the $C_1/C_2$ value of magma can be lower than that of the source (mantle) by no more than 10%, which is comparable with analytical errors for many elements, even ignoring the high natural scatter in element ratios (Table 1). For alkaline rocks produced by low-degree melting, the effect of incompatible element fractionation may be

**Table 1.** Ratios of the average concentrations of components in the magmatic melts of oceanic island (OI) and mid-ocean ridges (MOR)

| Component | Ratios of average concentrations | |
|---|---|---|
| | OI melts | MOR melts |
| $H_2O/Cl$ | 17 ± 16 | 24 ± 17 |
| $H_2O/F$ | 7.3 ± 7.0 | 19 ± 15 |
| $H_2O/P_2O_5$ | 1.6 ± 1.2 | 2.1 ± 1.7 |
| Cl/F | 0.4 ± 0.4 | 0.8 ± 0.3 |
| $K_2O/H_2O$ | 1.2 ± 0.9 | 0.5 ± 0.5 |
| $K_2O/Cl$ | 21 ± 16 | 11 ± 7 |
| $K_2O/F$ | 9.0 ± 6.9 | 8.7 ± 4.9 |
| $K_2O/P_2O_5$ | 2.0 ± 1.3 | 1.0 ± 1.0 |
| $TiO_2/H_2O$ | 4.5 ± 2.2 | 4.1 ± 2.2 |
| $TiO_2/Cl$ | 78 ± 47 | 95 ± 90 |
| $TiO_2/F$ | 33 ± 19 | 78 ± 35 |
| $TiO_2/K_2O$ | 3.6 ± 2.0 | 8.9 ± 8.4 |
| $TiO_2/P_2O_5$ | 7.3 ± 4.0 | 8.9 ± 5.1 |
| $P_2O_5/Cl$ | 11 ± 8 | 11 ± 12 |
| $P_2O_5/F$ | 4.5 ± 3.6 | 8.8 ± 6.8 |

more significant, and it is desirable to use only elements with similar *D* values in such a case.

The elements considered in this paper (K, Ce, Cl, F, and $H_2O$) are characterized by low *D* values; however, there are some differences among them. The lowest *D* values between mantle mineral assemblages and basaltic magmas are characteristic of potassium and chlorine (<0.01). Water is perhaps slightly more compatible ($D \sim 0.01$–$0.02$; Micheal, 1995; Hirth and Kohlstedt, 1996; Dixon et al., 1988) and similar to cerium. More compatible are fluorine ($D = 0.036$; Micheal, 1995; Schilling et al., 1980) and phosphorus ($D = 0.075$; Brunet and Chazot, 2001). Thus, it is reasonable to assume that the ratios of potassium to chlorine, water to cerium, and phosphorus to neodymium in basaltic magmas are identical to the respective mantle values. On the other hand, taking into account the uncertainties in the estimates of partition coefficients and relatively high degrees of melting during basaltic magma generation, it can be stated that the ratio of two elements whose *D* values differ from each other by 0.02 is also not strongly different from the ratio in their mantle sources (e.g., $Cl/H_2O$, $K_2O/H_2O$, F/Cl).

The compositions of glasses from basalts and melt inclusions characterize melts of different degrees of differentiation. The average compositions of basaltic magmas from ocean islands (Table 2) can be produced by the fractionation of up to 50% olivine from a melt in equilibrium with mantle olivine ($Fo_{88–90}$). The removal of such amounts of olivine should have a negligible effect on the ratios of incompatible elements, even if their *D* values differ by 0.03–0.05.

The above considerations led us to two conclusions, which are important for the understanding of the reliability of results obtained in our study: (1) the degree of incompatibility of the elements considered here (e.g., $K_2O$ and $H_2O$ or $K_2O$ and F) has a small influence on the difference of incompatible element ratios in sources and magmas, and this difference is much smaller than the natural dispersion of these ratios; (2) when necessary, the proportions of incompatible elements in magmas can be readily recalculated to the ratios in their source for any difference in the incompatibility of components using Eqs. (1) and (2) and Fig. 1.

## AVERAGE COMPOSITION OF OCEAN ISLAND MAGMAS AND THE ESTIMATION OF THE AVERAGE CONTENTS OF VOLATILE COMPONENTS IN THE PLUME MANTLE

Table 2 presents the average chemical composition of basic magmas from ocean islands (OI), including the concentrations of volatile components. These compositions were calculated for magmas containing up to 54 wt % $SiO_2$ in accordance with the histogram shown in Fig. 2. The geometric means of $H_2O$, Cl, F, Ti, P, Ce, and K concentrations were used, because these concentrations are more consistent with the lognormal rather than normal distribution (Fig. 3 and Kovalenko et al., 2006b). The average composition of OI magmas corresponds to a typical basalt slightly enriched in potassium, titanium, and phosphorus compared with the average composition of basaltic magmas from mid-ocean ridges (MOR) (Naumov et al., 2004; Kovalenko et al., 2006b) at a similar MgO content (slightly below 8 wt %). The average concentrations of major and trace elements (Table 3) in melt inclusions correspond to less differentiated magmas compared with quenched glasses. The geometric means of $H_2O$, Cl, and F contents in the basaltic magmas of OI are higher than in the basaltic magmas of MOR: $H_2O$, by a factor of less than 2; $K_2O$, by a factor of 4; Cl, by a factor of 2.5; and F, by a factor of more than 4. The average content of S in the basaltic magmas of OI is approximately 25% lower than that in MOR magmas (Kovalenko et al., 2006a).

Table 1 gives the ratios of the average contents of volatile components to each other and to the average concentrations of $K_2O$, $TiO_2$, and $P_2O_5$. As was noted above, these ratios in magmas must be equivalent, as a first approximation, to the respective characteristics of magma sources, i.e., must approach these ratios in mantle plumes. Despite the considerable natural variations, the average element ratios in basic magmas from OI and MOR are different, which suggests either different magma sources or different degrees of melting in these environments. On the other hand, there is a considerable overlap of these ratios in the MOR and OI magmas, which is also characteristic of isotopic parameters (Sr, Nd, and Hf) and ratios of highly incompatible

**Table 2.** Average concentrations of major, volatile, and trace elements in the magmatic melts of ocean islands and mid-ocean ridges

| Component | Mean concentrations in ocean island melts | | | Mean concentrations in mid-ocean ridge melts | | |
|---|---|---|---|---|---|---|
| | *n* | arithm | geom | *n* | arithm | geom |
| $SiO_2$ | 3447 | 50.24 | 50.23 | 3762 | 50.20 | 50.20 |
| | | 2.08 | 2.16–2.08 | | 0.92 | 0.93–0.92 |
| **$TiO_2$** | **3290** | **2.42** | **2.04** | **2596** | **1.34** | **1.24** |
| | | 0.84 | 0.92–0.63 | | 0.62 | 0.53–0.38 |
| $Al_2O_3$ | 3305 | 13.84 | 13.85 | 2525 | 15.59 | 15.58 |
| | | 1.55 | 1.67–1.49 | | 1.21 | 1.25–1.16 |
| FeO | 3341 | 10.72 | 10.66 | 2583 | 9.24 | 9.23 |
| | | 1.91 | 2.27–1.87 | | 1.65 | 1.71–1.43 |
| MnO | 2159 | 0.16 | 0.16 | 1450 | 0.16 | 0.16 |
| | | 0.07 | 0.07–0.05 | | 0.04 | 0.06–0.04 |
| MgO | 3424 | 7.30 | 7.33 | 2815 | 7.81 | 7.80 |
| | | 2.10 | 2.66–1.95 | | 1.43 | 1.58–1.32 |
| **CaO** | **3305** | **11.16** | **11.19** | **2525** | **11.54** | **11.54** |
| | | 1.49 | 1.85–1.59 | | 1.10 | 1.23–1.10 |
| **$Na_2O$** | **3290** | **2.35** | **2.32** | **2565** | **2.67** | **2.66** |
| | | 0.64 | 0.59–0.47 | | 0.57 | 0.64–0.51 |
| **$K_2O$** | **3340** | **0.51** | **0.56** | **3462** | **0.20** | **0.14** |
| | | 0.50 | 0.52–0.27 | | 0.27 | 0.30–0.10 |
| **$P_2O_5$** | **2899** | **0.28** | **0.28** | **2243** | **0.15** | **0.14** |
| | | 0.22 | 0.24–0.13 | | 0.12 | 0.16–0.07 |
| **$H_2O$** | **798** | **0.40** | **0.45** | **1051** | **0.29** | **0.30** |
| | | 0.36 | 0.55–0.25 | | 0.26 | 0.37–0.16 |
| **Cl** | **1385** | **320** | **270** | **1151** | **180** | **130** |
| | | 350 | 510–180 | | 260 | 450–100 |
| **F** | **839** | **650** | **620** | **341** | **180** | **160** |
| | | 760 | 1130–400 | | 170 | 210–90 |
| S | 1900 | 710 | 720 | 549 | 1010 | 990 |
| | | 630 | 1190–450 | | 420 | 480–320 |
| $CO_2$ | 576 | 180 | 110 | 455 | 190 | 150 |
| | | 310 | 330–80 | | 210 | 120–70 |
| Total | | 99.58 | 99.24 | | 99.19 | 98.99 |
| **Li** | **33** | **4.51** | **4.41** | **307** | **6.33** | **6.16** |
| | | 1.47 | 1.36–1.04 | | 2.22 | 1.82–1.40 |
| Be | 56 | 0.80 | 0.75 | 308 | 0.61 | 0.62 |
| | | 0.25 | 0.51–0.30 | | 0.38 | 0.38–0.24 |
| **B** | **84** | **1.33** | **1.22** | **193** | **1.86** | **1.61** |
| | | 1.10 | 1.12–0.58 | | 1.18 | 1.00–0.62 |
| **Sc** | **112** | **31.9** | **32.6** | **574** | **38.5** | **38.4** |
| | | 8.6 | 11.9–8.7 | | 5.3 | 6.0–5.1 |
| V | 262 | 274 | 262 | 546 | 269 | 267 |
| | | 140 | 147–94 | | 65 | 77–64 |
| Cr | 685 | 485 | 382 | 858 | 303 | 299 |
| | | 624 | 690–250 | | 198 | 239–133 |
| Co | 44 | 49.8 | 50.4 | 216 | 44.8 | 44.8 |
| | | 7.7 | 10.2–8.5 | | 5.4 | 5.5–4.9 |
| **Ni** | **317** | **226** | **176** | **399** | **97.5** | **97.5** |
| | | 220 | 270–110 | | 48.0 | 54.2–34.8 |
| **Rb** | **155** | **10.1** | **8.61** | **500** | **4.01** | **1.53** |
| | | 13.1 | 8.68–4.32 | | 6.85 | 3.71–1.08 |
| **Sr** | **493** | **259** | **232** | **803** | **135** | **130** |
| | | 257 | 360–140 | | 65 | 62–44 |

**Table 2.** (Contd.)

| Component | Mean concentrations in ocean island melts | | | Mean concentrations in mid-ocean ridge melts | | |
|---|---|---|---|---|---|---|
| | *n* | arithm | geom | *n* | arithm | geom |
| **Y** | **361** | **20.4** | **19.6** | **796** | **28.1** | **28.0** |
| | | 12.2 | 17.1–9.1 | | 13.1 | 12.7–8.7 |
| Zr | 476 | 92.0 | 83.8 | 929 | 93.7 | 90.2 |
| | | 85.0 | 166–58 | | 53.1 | 74.9–40.9 |
| **Nb** | **324** | **17.4** | **10.2** | **763** | **4.84** | **2.37** |
| | | 32.3 | 13.0–5.7 | | 6.89 | 4.36–1.54 |
| **Ba** | **357** | **80.6** | **62.9** | **654** | **30.6** | **16.6** |
| | | 110 | 160–45 | | 52.8 | 57.0–12.9 |
| La | 529 | 8.26 | 3.58 | 1065 | 5.51 | 4.38 |
| | | 14.4 | 9.71–2.61 | | 5.98 | 5.71–2.48 |
| Ce | 415 | 18.0 | 9.16 | 1175 | 12.5 | 11.2 |
| | | 30.8 | 32.6–7.2 | | 10.9 | 13.3–6.1 |
| **Pr** | **87** | **3.84** | **4.34** | **181** | **2.12** | **1.73** |
| | | 2.06 | 1.53–1.16 | | 1.69 | 1.35–0.76 |
| Nd | 415 | 10.6 | 7.35 | 874 | 10.6 | 10.4 |
| | | 13.4 | 19.7–5.4 | | 5.9 | 7.0–4.2 |
| **Sm** | **432** | **3.12** | **2.35** | **952** | **3.57** | **3.45** |
| | | 3.16 | 4.05–1.49 | | 1.88 | 1.68–1.21 |
| Eu | 394 | 1.23 | 0.98 | 793 | 1.28 | 1.21 |
| | | 1.18 | 1.50–0.59 | | 0.61 | 0.51–0.36 |
| **Gd** | **150** | **5.86** | **5.89** | **547** | **4.42** | **4.36** |
| | | 2.18 | 2.33–1.67 | | 1.46 | 1.55–1.14 |
| Tb | 39 | 0.93 | 0.91 | 246 | 0.74 | 0.78 |
| | | 0.29 | 0.22–0.18 | | 0.26 | 0.27–0.20 |
| **Dy** | **414** | **3.56** | **3.40** | **779** | **4.82** | **4.74** |
| | | 2.34 | 3.19–1.64 | | 2.06 | 2.01–1.41 |
| Ho | 85 | 1.07 | 1.05 | 170 | 1.01 | 0.98 |
| | | 0.13 | 0.12–0.11 | | 0.34 | 0.34–0.25 |
| **Er** | **405** | **2.11** | **1.98** | **637** | **3.05** | **3.00** |
| | | 1.18 | 1.34–0.81 | | 1.25 | 1.13–0.82 |
| Tm | 39 | 0.46 | 0.45 | 173 | 0.41 | 0.40 |
| | | 0.08 | 0.09–0.07 | | 0.14 | 0.14–0.10 |
| **Yb** | **526** | **1.89** | **1.81** | **817** | **2.98** | **2.90** |
| | | 0.91 | 0.91–0.61 | | 1.35 | 1.26–0.88 |
| **Lu** | **81** | **0.33** | **0.34** | **455** | **0.45** | **0.43** |
| | | 0.07 | 0.09–0.07 | | 0.20 | 0.15–0.11 |
| **Hf** | **118** | **3.56** | **3.71** | **398** | **2.39** | **2.31** |
| | | 1.09 | 1.39–1.00 | | 1.07 | 1.19–0.79 |
| **Ta** | **80** | **0.89** | **0.90** | **370** | **0.30** | **0.28** |
| | | 0.28 | 0.34–0.25 | | 0.41 | 0.55–0.19 |
| Pb | 84 | 0.89 | 1.02 | 326 | 0.71 | 0.73 |
| | | 0.61 | 0.81–0.46 | | 0.53 | 0.41–0.26 |
| **Th** | **94** | **0.64** | **0.66** | **525** | **0.46** | **0.37** |
| | | 0.52 | 1.00–0.40 | | 0.74 | 0.78–0.25 |
| **U** | **84** | **0.26** | **0.21** | **397** | **0.16** | **0.10** |
| | | 0.10 | 0.40–0.14 | | 0.26 | 0.21–0.06 |

Note: Here and in Tables 3 and 5, the concentrations of major components and water are given in wt %, and other elements are in ppm; *n* is the number of determinations; arithm is the arithmetic mean with standard deviations beneath the values; geom is the geometric mean with standard deviations beneath the values (first number shows the positive deviation, and the second number is the negative deviation). The concentrations of elements are calculated as arithmetic and geometric means, and the maximum deviation of an individual measurement from the average value is no higher than $2\sigma$ with a probability of 95%. The components shown in bold are characterized by significant (at a 99% level) differences between OI and MOR magmas, taking into account possible variations in the degree of fractionation (up to 20% of silicate phases and small amounts of spinel and sulfide melt).

refractory components (Hofmann, 2003). If the concentration of any of the aforementioned elements in the plume mantle is known, the concentrations of all other incompatible elements can be readily calculated from respective ratios. To our knowledge, the average contents of the elements in mantle plumes are not reliably known, although some estimates for particular regions have recently been reported (Dixon et al., 2001, 2002; Simons et al., 2002).

In many physical models, mantle plumes are considered as primarily thermal phenomena originating in high-temperature mantle zones. If the thermal nature of mantle plumes is accepted, it is reasonable to suppose that the average concentrations of nonvolatile components (including potassium, titanium, and phosphorus) in them must be similar to the average concentrations of these elements in the MOR mantle. Then, the average concentration of $K_2O$ in the plume mantle must be 72 ppm (McDonough et al., 1992). Using the results of simultaneous determination of potassium and volatile components, the following average contents can be obtained for the plume mantle: 73 ppm $H_2O$, 2.9 ppm Cl, and 7.7 ppm F (Table 4). The average contents of $H_2O$ and Cl are two times lower than the estimates for the MOR mantle (158 ppm $H_2O$ and 6.6 ppm Cl; Kovalenko et al., 2006a). The average F content in the plume mantle (7.7 ppm) for this model is approximately equal to that of the MOR mantle (8.3 ppm). Such relationships of element concentrations in the depleted mantle (DM) and plume mantle are possible, if the OI magmas are formed at lower degrees of melting compared with the MOR magmas. For example, if the average degree of melting (more precisely, the combined effect of the degree of melting and the degree of differentiation expressed as $C_s/C_m$, where $C_s$ is the concentration in the source, and $C_m$ is the concentration in the magma) is 0.055 for the MOR magmas, the average degree of melting for the OI magmas is 0.013, i.e., lower by a factor of 4. Now the question is why the degree of melting of the isochemical mantle is lower in high-temperature plumes than in the enclosing colder MOR mantle.

The average concentrations of the elements in the plume mantle can be estimated through the average concentration of Ce in this reservoir, because the incompatibility of this element is similar to that of $H_2O$ (Dixon et al., 2002). These authors estimated that the abundance of Ce is 3 ppm in the FOZO mantle source of the Atlantic, 3.8 ppm in the Pacific Ocean mantle, and 4 ppm in the EM source. Accepting an intermediate value of 3.8 ppm, the average concentrations of elements in the plume mantle can be calculated from the average ratios in OI magmas (Table 2): $K_2O/Ce = 611$, $H_2O/Ce = 491$, $Cl/Ce = 29$, and $F/Ce = 68$. The obtained concentrations of the elements are about an order of magnitude higher than those calculated for the model of thermal plumes: 2322 ppm $K_2O$, 1866 ppm $H_2O$, 110 ppm Cl, and 258 ppm F. Such concentrations of volatile components and $K_2O$ in the plume mantle suggest a degree of melting of 0.38 for the formation of OI magmas (Tables 1, 2), which is probably an overestimation.

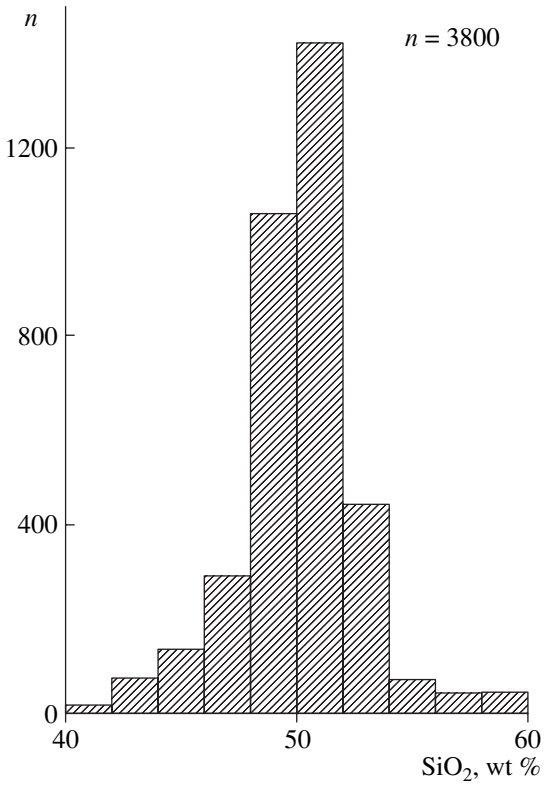


**Fig. 2.** Histogram showing the distribution of $SiO_2$ contents in the natural magmatic melts of ocean islands. $n$ is the number of determinations.

The average content of S in the plume mantle can be estimated assuming that the average concentration of Dy in the plume mantle is identical to that of the MOR mantle (0.531 ppm). For S/Dy = 212 in the OI magmas, the average content of S in the plume mantle is 140 ppm, which is not very different from the content of S in the DM. Another estimate can be obtained from the equation $C^0 = C(1 - F)^{D-1}$, where $C^0$ is the concentration of S in the source, $C$ is the concentration of S in the magma in equilibrium with the source, $(1 - F)$ is the degree of melting, and $D$ is the bulk partition coefficient of S between crystals and melt. Taking $D = 0.114$ (Kovalenko et al., 2006c) and $(1 - F) = 0.38$, we obtain $C^0 =$ 378 ppm. This model is questionable because of the unrealistically large melt fraction. Accepting a degree of melting of 0.08 for the OI magmas (Simons et al., 2002) and using $D$ values after Workman and Hart (2005), the average concentrations of nonvolatile Ce and $K_2O$ in the plume mantle can be estimated as 0.84 and 462 ppm, respectively. The average concentrations of volatile components in the plume mantle calculated from the concentrations of Ce and $K_2O$ are, respectively, 412 and 575 ppm $H_2O$, 25 and 22 ppm Cl, and 57 and 51 ppm F (Table 2).

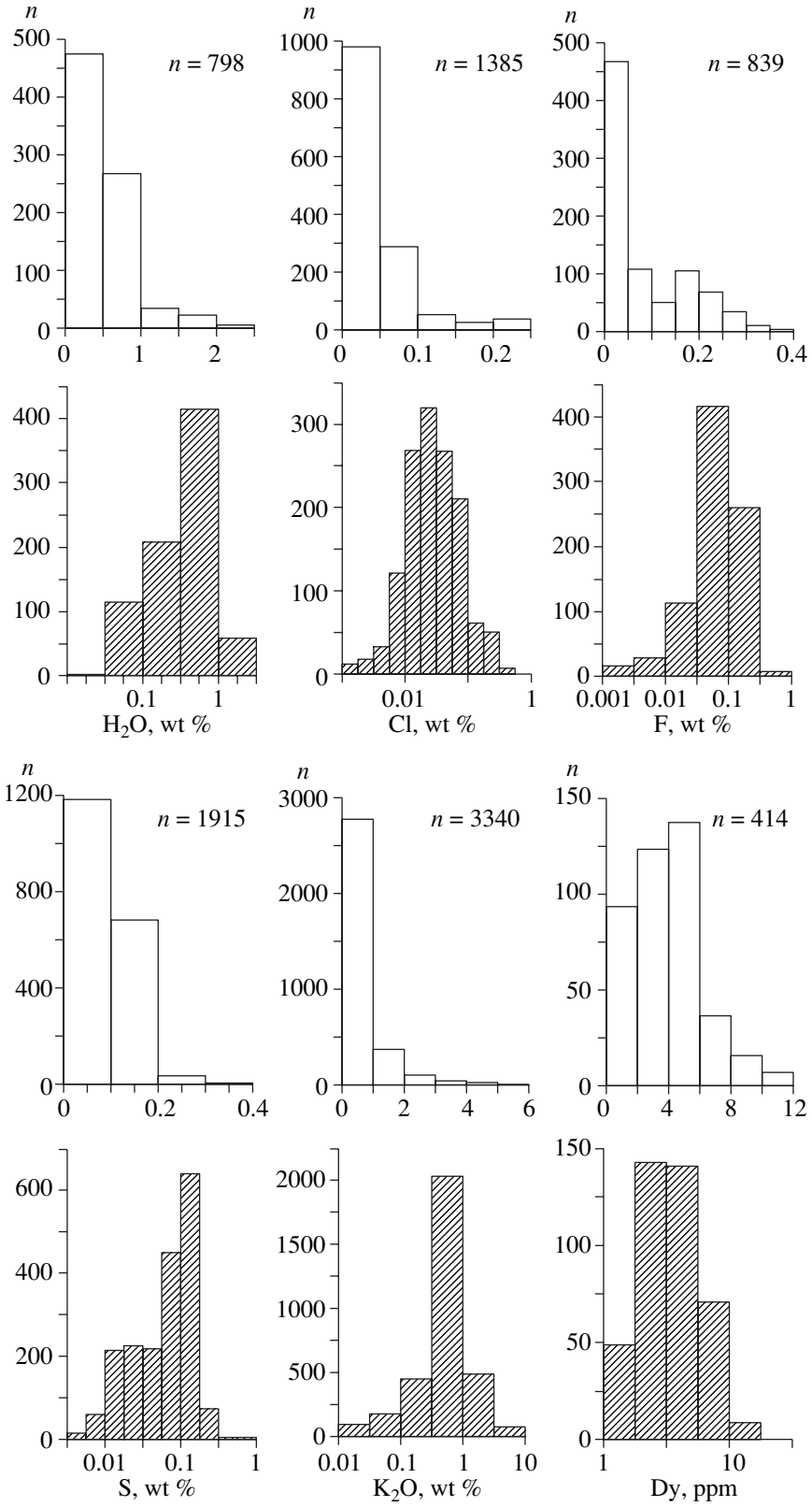


**Fig. 3.** Histograms showing the distribution of the contents of $H_2O$, Cl, F, S, $K_2O$, Dy, $P_2O_5$, $TiO_2$, and Ce in the magmatic melts of ocean islands. The unshaded and shaded histograms are drawn on linear and logarithmic scales to test for the normal and lognormal distribution, respectively. *n* is the number of determinations.

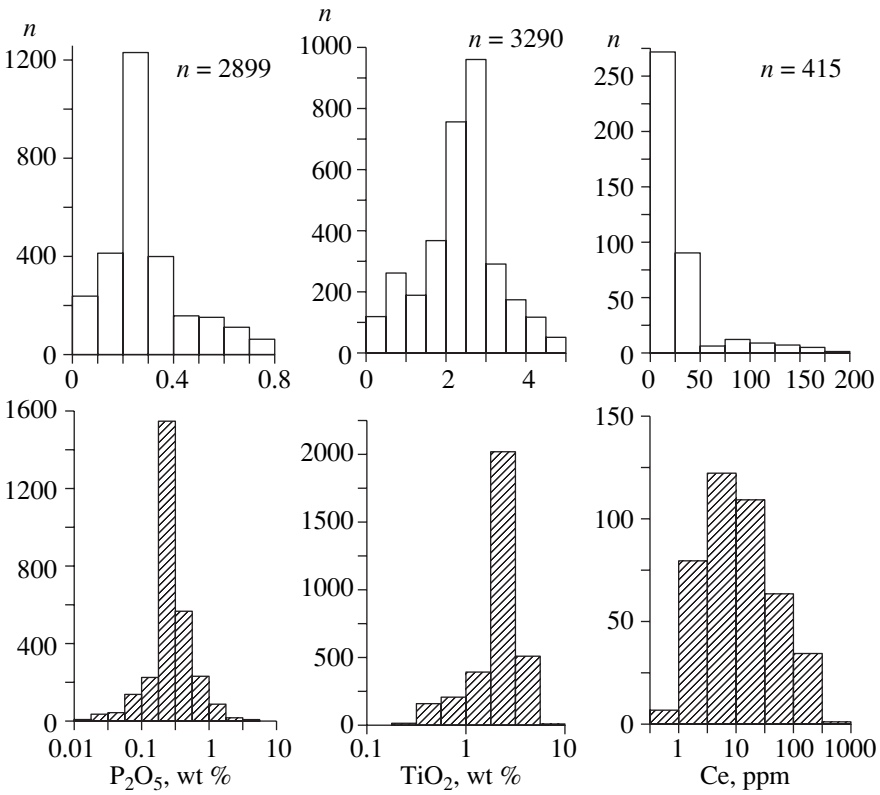


**Fig. 3.** (Contd.)

Using average ratios of elements with similar incompatibilities ($H_2O$/Ce, $K_2O$/Cl, and $P_2O_5$/F) (Saal et al., 2002; Salters and Stracke, 2004), the following average concentrations can be obtained for the plume mantle: 520 ppm $H_2O$, 21 ppm Cl, and 55 ppm F. All the calculated contents of volatile components in mantle plumes are somewhat higher than those in the DM. Such a model implies that the plume mantle is moderately enriched, which results in a smaller temperature difference from the enclosing depleted mantle. The obtained average content of water in the plume mantle is similar to the estimate for the KEA + KOO source of basic glasses from Loihi (400 ppm) and Kilauea Volcano (450 ± 190 ppm) of the Hawaiian Islands (Dixon and Clague, 2001).

Similar to the volatile components, the average concentrations of incompatible trace elements in the plume mantle were calculated for the models of thermal plumes and a moderately enriched source (Table 4).

The two models yield significantly different average concentrations of volatile and trace elements in the plume mantle (Table 4). Figure 4 shows the primitive mantle-normalized average concentrations of elements. There are negative anomalies in water and chlorine for both models, and the $H_2O$/Ce and $K_2O$/Cl ratios are identical. The spidergram pattern of the average mantle composition for the thermal plume model lies below the line of the primitive mantle and mostly below the DM composition (except for $K_2O$, Nb, and Ba) (Kovalenko et al., 2006c; Salters and Stracke, 2004). This is in conflict with the isotopic parameters of OI basalts, which are on average closer to those of the primitive mantle than to MOR basalts (Hofmann, 2003). This leads us to favor the model of an enriched source, taking into account that the degree of melting estimated for this model is more realistic than that for the isochemical mantle model. Note also the depletion of water relative to the neighboring elements in the spider diagram (Fig. 4), which is contrary to the idea of the high water content in the source of OI magmas (wet plumes).

Thus, the following values were obtained as the most probable average concentrations for the plume mantle: 510 ppm $K_2O$, 520 ppm $H_2O$, 21 ppm Cl, 55 ppm F, and 83 ppm S (Table 4, Fig. 4), which are significantly higher than those of the DM (Kovalenko et al., 2006c), except for the lower content of S in the plume mantle. The plume mantle is richer in $K_2O$ and F than the primitive mantle (Palme and O'Neill, 2003). Thus, the plume mantle can be considered as moderately enriched in potassium, volatile components, and incompatible trace elements compared with the DM but similar in the concentrations of these components to the primitive mantle.

It should be kept in mind that the obtained estimates are average characteristics blurring the chemical heterogeneity of the mantle. These estimates have the same

**Table 3.** Average concentrations of major, volatile, and trace elements in melt inclusions in minerals and quenched glasses from the igneous rocks of ocean islands

| Component | Melt inclusions | | | Quenched glasses | | |
|---|---|---|---|---|---|---|
| | *n* | arithm | geom | *n* | arithm | geom |
| $SiO_2$ | 1696 | 50.04 | 50.03 | 1751 | 50.40 | 50.39 |
| | | 2.04 | 2.10–2.01 | | 2.09 | 2.17–2.07 |
| $TiO_2$ | 1635 | 2.03 | 1.56 | 1655 | 2.65 | 2.61 |
| | | 1.02 | 1.09–0.64 | | 0.62 | 0.68–0.53 |
| $Al_2O_3$ | 1650 | 13.86 | 13.83 | 1655 | 13.87 | 13.86 |
| | | 2.02 | 2.15–1.86 | | 1.00 | 1.08–1.00 |
| FeO | 1684 | 9.93 | 9.90 | 1657 | 11.26 | 11.25 |
| | | 2.28 | 2.64–2.08 | | 1.18 | 1.41–1.24 |
| MnO | 1221 | 0.14 | 0.14 | 938 | 0.18 | 0.19 |
| | | 0.05 | 0.06–0.04 | | 0.06 | 0.05–0.04 |
| MgO | 1684 | 8.43 | 8.39 | 1740 | 6.54 | 6.49 |
| | | 2.32 | 2.85–2.13 | | 1.46 | 1.77–1.40 |
| CaO | 1650 | 11.58 | 11.63 | 1655 | 10.99 | 10.95 |
| | | 2.00 | 2.43–2.00 | | 1.12 | 1.37–1.22 |
| $Na_2O$ | 1635 | 2.22 | 2.20 | 1655 | 2.52 | 2.45 |
| | | 0.58 | 0.55–0.44 | | 0.74 | 0.64–0.51 |
| $K_2O$ | 1600 | 0.48 | 0.48 | 1740 | 0.55 | 0.59 |
| | | 0.49 | 0.68–0.28 | | 0.56 | 0.42–0.25 |
| $P_2O_5$ | 1336 | 0.26 | 0.26 | 1563 | 0.29 | 0.27 |
| | | 0.21 | 0.34–0.15 | | 0.21 | 0.13–0.09 |
| $H_2O$ | 293 | 0.35 | 0.34 | 505 | 0.42 | 0.49 |
| | | 0.36 | 0.71–0.23 | | 0.34 | 0.45–0.23 |
| Cl | 512 | 230 | 190 | 873 | 380 | 310 |
| | | 260 | 400–130 | | 390 | 540–190 |
| F | 326 | 600 | 570 | 513 | 770 | 720 |
| | | 570 | 730–330 | | 990 | 1680–510 |
| S | 620 | 980 | 950 | 1295 | 620 | 560 |
| | | 710 | 820–440 | | 620 | 1260–390 |
| $CO_2$ | 226 | 210 | 130 | 350 | 130 | 90 |
| | | 380 | 430–100 | | 230 | 210–60 |
| Be | 24 | 0.77 | 0.75 | 32 | 0.85 | 0.88 |
| | | 0.22 | 0.30–0.22 | | 0.26 | 0.29–0.22 |
| B | 61 | 1.26 | 1.07 | 23 | 1.59 | 1.44 |
| | | 1.16 | 1.54–0.63 | | 0.82 | 0.74–0.49 |
| V | 107 | 195 | 192 | 155 | 312 | 317 |
| | | 84 | 91–62 | | 83 | 108–81 |
| Cr | 423 | 647 | 494 | 262 | 236 | 237 |
| | | 776 | 963–327 | | 194 | 310–134 |
| Ni | 55 | 383 | 334 | 262 | 172 | 140 |
| | | 375 | 409–184 | | 147 | 181–79 |
| Sr | 297 | 198 | 177 | 196 | 314 | 273 |
| | | 199 | 334–115 | | 273 | 312–145 |
| Y | 186 | 13.1 | 12.8 | 175 | 27.6 | 27.6 |
| | | 6.6 | 6.7–4.4 | | 7.9 | 9.0–6.8 |

**Table 3.** (Contd.)

| Component | Melt inclusions | | | Quenched glasses | | |
|---|---|---|---|---|---|---|
| | *n* | arithm | geom | *n* | arithm | geom |
| Zr | 283 | 70.0 | 48.9 | 193 | 124 | 124 |
| | | 80.5 | 145–36.6 | | 70 | 80–49 |
| Nb | 156 | 10.9 | 9.3 | 168 | 18.1 | 10.8 |
| | | 10.1 | 7.7–4.2 | | 38.6 | 13.6–6.0 |
| Ba | 211 | 56.2 | 56.6 | 146 | 102 | 77.0 |
| | | 63.8 | 155–42 | | 172 | 184–54 |
| La | 342 | 4.62 | 2.30 | 187 | 11.7 | 9.4 |
| | | 6.99 | 5.30–1.61 | | 18.9 | 12.2–5.3 |
| Ce | 230 | 6.27 | 3.37 | 185 | 26.1 | 22.7 |
| | | 13.8 | 5.15–2.04 | | 27.6 | 24.9–11.9 |
| Nd | 230 | 5.10 | 3.19 | 185 | 16.6 | 15.9 |
| | | 8.84 | 3.76–1.73 | | 11.0 | 13.7–7.4 |
| Sm | 245 | 1.89 | 1.26 | 187 | 4.48 | 4.49 |
| | | 2.53 | 0.80–0.49 | | 2.36 | 2.61–1.65 |
| Eu | 227 | 0.90 | 0.67 | 167 | 1.67 | 1.55 |
| | | 1.22 | 0.54–0.30 | | 0.64 | 0.64–0.45 |
| Dy | 230 | 2.54 | 2.25 | 184 | 4.89 | 4.94 |
| | | 1.80 | 1.58–0.93 | | 1.36 | 1.61–1.22 |
| Er | 230 | 1.69 | 1.53 | 175 | 2.66 | 2.64 |
| | | 0.99 | 0.86–0.55 | | 0.74 | 0.86–0.65 |
| Yb | 340 | 1.72 | 1.61 | 186 | 2.22 | 2.22 |
| | | 0.79 | 0.78–0.52 | | 0.71 | 0.79–0.59 |
| Hf | 22 | 3.82 | 3.42 | 96 | 3.71 | 3.73 |
| | | 1.94 | 2.66–1.50 | | 0.63 | 0.81–0.67 |

meaning as any other global chemical characteristics of the Earth's interiors. The real mantle is of course heterogeneous, which is supported by numerous lines of evidence based on the isotopic and trace element systematics of mantle magmas and nodules (Hofmann, 2003). The heterogeneity of the plume mantle with respect to volatile components is discussed below.

## COMPOSITIONAL HETEROGENEITY OF OCEAN ISLAND MAGMAS AND PLUME MANTLE

The analysis of our database indicated that the OI magmas are heterogeneous and show no general correlation between the concentrations of $H_2O$ and $K_2O$ or $H_2O$ and Ce. The evaluation of the heterogeneity of the plume mantle is based on the correlations between the concentrations of $K_2O$, Ce, $H_2O$, $TiO_2$, and $P_2O_5$ in the OI magmas (Kovalenko et al., 2006b). The compositions of OI magmas form three groups in the $K_2O$–$H_2O$ and $TiO_2$–$H_2O$ diagrams (Fig. 5). Group I has a low potassium content and is similar to the tholeiitic series of MOR basic magmas. Group II is highly potassic and approaches the subalkaline and alkaline series of intraplate continental geodynamic settings (continental rifts and hot spots, CR). Compositional fields I and II overlap in the region of high water and potassium contents (Fig. 5), where group III is distinguished, also similar to CR magmas. The boundary between fields I and II + III corresponds to a $K_2O$ content of 0.2 wt %. Similar relations can be observed in the Ce–$H_2O$ and $P_2O_5$–$H_2O$ diagrams (Kovalenko et al., 2006a). Thus, there are three main groups of the compositions of OI basic magmas: (I) low-potassium, poor in P and Ti, and similar to MOR magmas; (II) high-potassium, rich in Ce, P, and Ti, and similar to the basic magmas of CR, except for the lower water content; and (III) high-potassium and enriched in Ce, P, Ti, and water. The concentration ratios $K_2O/H_2O$, $Ce/H_2O$, $TiO_2/H_2O$, and $P_2O_5/H_2O$ decrease from field II to fields I + III.

Figure 6 shows the compositions of OI magmas in the $SiO_2$–$K_2O$ diagram. The compositions of field I magmas correspond to low-potassium tholeiitic basalts, and the compositions of fields II + III correspond to

**Table 4.** Average concentrations of elements (ppm) in the sources of mantle plume magmas from ocean islands calculated on the basis of two models

| Component | Bulk average content | *n* | Component | Bulk average content | *n* |
|---|---|---|---|---|---|
| Thermal model | | | Model of enriched source | | |
| $K_2O$ | 72 | | $K_2O$ | 510 | |
| $H_2O$ | 73 (+82/–39) | 787 | $H_2O$ | 520 (+590/–270) | 787 |
| Cl | 2.9 (+3.2/–1.5) | 1400 | Cl | 21 (+23/–11) | 1400 |
| F | 7.7 (+5.1/–3.1) | 839 | F | 55 (+36/–22) | 839 |
| S | 12 (+25/–8.0) | 1909 | S | 83 (+180/–57) | 1909 |
| $TiO_2$ | 371 (+257/–152) | 3206 | $TiO_2$ | 2600 (+1800/–1100) | 3206 |
| $P_2O_5$ | 44 (+18/–12) | 2894 | $P_2O_5$ | 310 (+130/–90) | 2894 |
| Sr | 6.1 (+5.4/–2.8) | 446 | Sr | 43 (+38/–20) | 446 |
| Y | 0.7 (+2.1/–0.5) | 316 | Y | 5.1 (+1.5/–3.8) | 316 |
| Zr | 2.7 (+2.2/–1.2) | 429 | Zr | 19 (+15/–8) | 429 |
| Nb | 0.21 (+0.13/–0.08) | 320 | Nb | 1.5 (+0.9/–0.6) | 320 |
| Ba | 1.5 (+0.6/–0.4) | 319 | Ba | 11 (+4/–3) | 319 |
| La | 0.20 (+0.12/–0.07) | 439 | La | 1.4 (+0.8/–0.5) | 439 |
| Ce | 0.56 (+0.38/–0.23) | 325 | Ce | 3.9 (+2.7/–1.6) | 325 |
| Nd | 0.40 (+0.44/–0.21) | 325 | Nd | 2.8 (+3.1/–1.5) | 325 |
| Sm | 0.12 (+0.19/–0.07) | 342 | Sm | 0.83 (+1.33/–0.51) | 342 |
| Eu | 0.04 (+0.06/–0.02) | 304 | Eu | 0.25 (+0.43/–0.16) | 304 |
| Dy | 0.13 (+0.33/–0.09) | 324 | Dy | 0.92 (+2.31/–0.66) | 324 |
| Yb | 0.04 (+0.11/–0.03) | 436 | Yb | 0.30 (+0.77/–0.21) | 436 |

Note: *n* is the number of determinations. Numbers in parentheses show the deviations from the average values.

potassium-rich basalts characterized by a decrease in $SiO_2$ content with increasing $K_2O$.

The distribution of other volatile components in the basaltic magmas of fields I, II, and III was considered in detail by Kovalenko et al. (2006b), and only main conclusions concerning the behavior of these components and selected regression equations for their concentrations are presented here. With respect to F and $K_2O$ concentrations, the compositions of fields I and II and high-F compositions of field III define a common linear array on a logarithmic scale ($\log F = 0.8 \log K_2O - 1.1$, $R^2 = 0.38$), which is close to the combined trend of the compositions of MOR and CR. The average $K_2O/F$ ratio of OI basalts is about 9. The concentration of F in the compositions of filed III is strongly variable at slightly varying $K_2O$ concentrations, whereas the compositions of fields II and III practically coincide in the $K_2O$–F diagram. Almost all magmas with more than 0.05 wt % fluorine are potassium-rich ($K_2O > 0.2$ wt %).

The concentrations of F and $P_2O_5$ (according to many authors, they have similar compatibilities) form a statistically significant correlation: $\log P_2O_5 = 0.38 \log F + 0.03$, $R^2 = 0.39$. The compositions of fields II and III also show a common positive correlation with an increase in $P_2O_5$ and F concentrations from the MOR field to CR. The $P_2O_5/F$ ratio declines systematically with increasing fluorine content: $\log(P_2O_5/F) = -0.62 \log F + 0.03$, $R^2 = 0.63$. There is no correlation between F and Cl, either for the whole data set of OI basalts or for particular fields.

With respect to Cl and $K_2O$, two groups of OI magmas were distinguished with strongly variable Cl contents (Kovalenko et al., 2006b): low-potassium compositions ($K_2O < 0.2$ wt %) of field I and high-potassium compositions ($K_2O > 0.2$ wt %) of fields II and III. Both these groups form an elongated ellipse overlapping the compositions of the basaltic magmas of MOR and CR. The $Cl/K_2O$ ratio varies from <0.01 to >1. The linear regression of the whole data set gives $\log Cl = 0.95 \log K_2O - 1.09$, $R^2 = 0.39$. The compositions of potassium-rich fields II and III form a less steep correlation, and the $Cl/K_2O$ ratio varies from <0.01 to 0.1 in field II and from 0.1 to >1 in field III. A similar correlation was observed for Cl and $H_2O$. The compositions of OI basaltic magmas fall within the field of the basaltic magmas of MOR and extend toward the basaltic magmas of CR with higher $H_2O$ and Cl contents. The

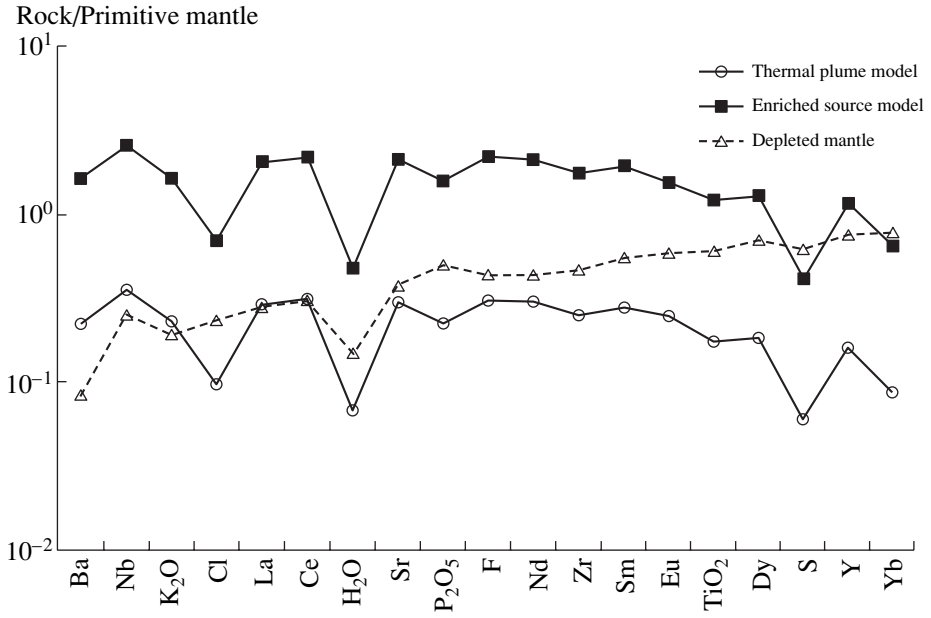


**Fig. 4.** Primitive mantle-normalized (Palme and O'Neill, 2003) average concentrations of K, volatile components, and incompatible trace elements in the plume mantle estimated on the basis of the models of thermal mantle and moderately enriched sources. Also shown is the average composition of the depleted mantle (source of mid-ocean ridge basalts) (Workman and Hart, 2005).

$H_2O$/Cl ratio decreases from ~100 to <10, averaging 17 (Table 1), which is lower than that of seawater.

In the $K_2O$–$P_2O_5$, $P_2O_5$–$TiO_2$, $K_2O$–$TiO_2$, and $K_2O$–Ce diagrams, field II coincides with field III, and all the compositions of OI basaltic magmas form common positive correlations. Field I is situated in the region of low K, Ti, and P concentrations, whereas fields II and III are characterized by high concentrations of these elements (Kovalenko et al., 2006b).

The calculated average compositions of the three groups of OI magmas are given in Table 5. The low-potassium compositions of group I resemble MOR magmas (Table 2) with respect to other major oxides, differing in lower $TiO_2$, $K_2O$, $P_2O_5$, and $H_2O$ and higher CaO and Fe contents. The average compositions of group II and III magmas differ from the average composition of group I in higher concentrations of $TiO_2$, $K_2O$, and $P_2O_5$. Compared with the compositions of field III, the average composition of field II magmas shows lower contents of $H_2O$, Cl, and S (but not F).

Table 6 presents the average ratios of volatile and nonvolatile components in magmas, which are used together with Table 5 to estimate the compositions of the sources of these magmas, i.e., the plume mantle. However, it is necessary first to estimate possible changes in these parameters (Fig. 5; Tables 1, 2) due to shallow crustal processes. The observed correlations between volatile and nonvolatile components, for instance, Cl with $K_2O$, F with $K_2O$, and F with $P_2O_5$, suggest that the behavior of all these incompatible components are controlled by common processes. The most important among such processes are crystallization differentiation, anatectic melting, and mixing of magmas or their sources. These processes may be responsible for the observed global correlations. The processes of assimilation and magma degassing must disturb the correlations between components. Therefore, if these processes occurred, their influence was subordinate compared to the existing global correlations. A comparison of the average compositions of group I, II, and III melts (Table 5) and average element ratios (Table 1) shows that the concentrations of MgO in them are similar, and crystal differentiation could not therefore be responsible for the sharp differences in the average contents of volatile components and, even more so, their ratios to the concentrations of nonvolatile components. It could have been suggested that the compositions of field II were formed by degassing of field III magmas (Fig. 5). However, since the content of water estimated for the magmas of these fields is very low (especially, for field II), this process had to occur practically at 1 atm, although such magmas were erupted on the ocean floor and trapped as melt inclusions at pressures of up to several kilobars. Consequently, magma degassing could not be the reason for the observed difference between the compositions of group II and III magmas. The degrees of melting for fields II and III were probably also similar, which is suggested by the similar correlations of $K_2O$ and $SiO_2$ in the magmas (Fig. 6, Table 5). Therefore, the differences between the average contents (Table 5) and ratios of volatile components (Table 1) are probably related to different compositions of the sources of these three magma types.

The possibility of oceanic basalt contamination by brines formed through seawater boiling has been dis-

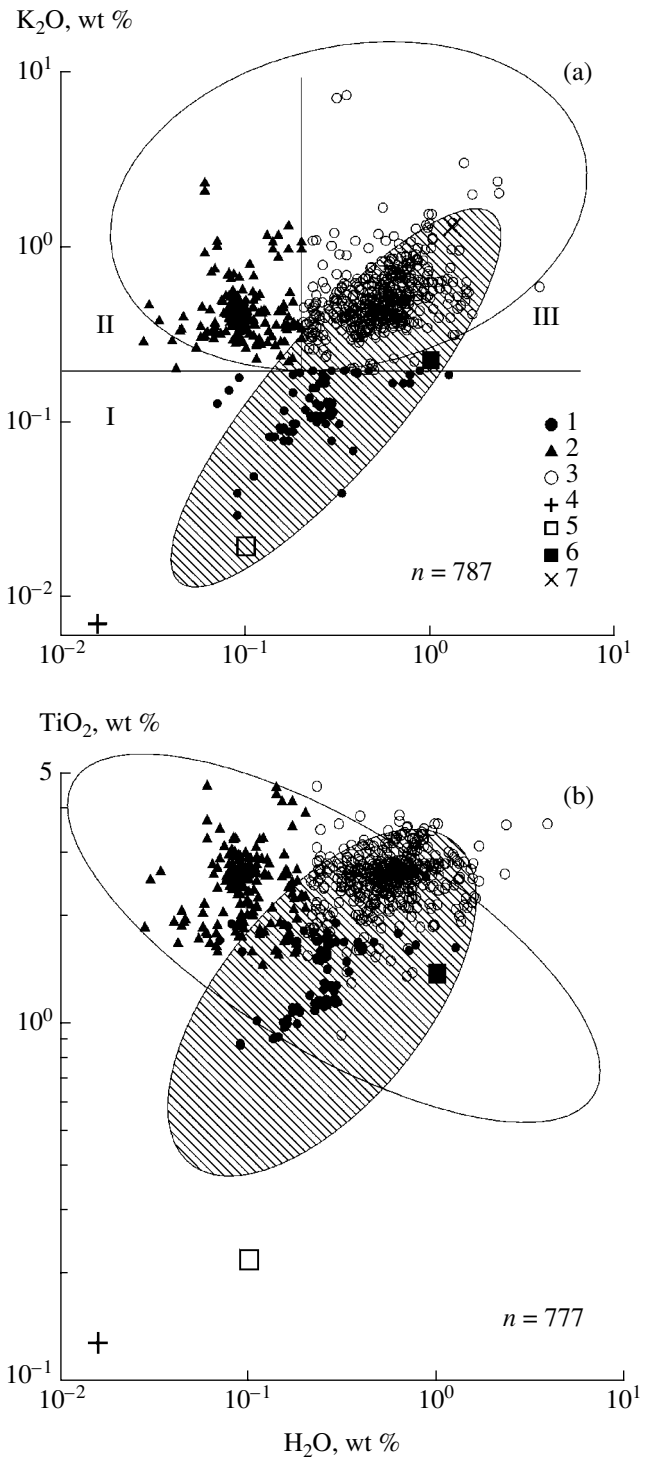


**Fig. 5.** Covariations of (a) $K_2O$ and $H_2O$ and (b) $TiO_2$ and $H_2O$ in the magmatic melts of ocean islands. (1) Low-potassium melts with $K_2O < 0.2$ wt % (field I); (2) high-potassium melts with $K_2O > 0.2$ wt % and low $H_2O$ content (<0.2 wt %, field II); (3) high-potassium melts with $K_2O >$ 0.2 wt % and high $H_2O$ content (>0.2 wt %, field III); (4) depleted mantle; (5) primitive mantle; (6) oceanic crust; and (7) continental crust. Here and in Figs. 6 and 8–12, the shaded ellipses indicate the fields of mid-ocean ridge melts, and the unshaded ellipses are the fields of magmatic melts from continental rifts and hot spots.

cussed in a number of publications. Thus, it could be supposed that some magmas from our database are enriched in Cl at the expense of such contamination (Kovalenko et al., 2002, 2006b). Let us estimate the probability of this process for OI magmas and the extent of its influence on the compositions of magmas on a global scale. The general positive correlations of Cl contents with $K_2O$ and $H_2O$ on a logarithmic scale (Kovalenko et al., 2006b) cannot be related to the assimilation of seawater components, including brines, because this process would have resulted in an increase in Cl at constant $K_2O$ and decreasing $H_2O$ contents, which was shown for a number of complexes (Dixon and Clague, 2001; Lassiter et al., 2002). The observed correlation is most likely related to mixing between two magma sources, poor and rich in Cl, $K_2O$, and $H_2O$ (Kovalenko et al., 2004). The assimilation of Cl-rich seawater components by OI magmas could produce a considerable scatter in Cl contents at a constant $K_2O$ concentration within the general correlation (indeed, Cl content varies over two orders of magnitude). This supposition is disputable, because the compositions of the magmas cluster near the average composition. The doubts are strengthened by the analysis of correlation between Cl and $K_2O$ concentrations in the magmas of fields II and III. This correlation could be attributed to the significant role of chloride brine assimilation, but in such a case it should be admitted that this process was responsible for the transition from group II to group III compositions. This is improbable, because this transition is also accompanied by an increase in the concentrations of $K_2O$, $H_2O$, S, and presumably $TiO_2$ (Table 2). It should be noted that type III magmas may contain up to 2 wt % Cl at low concentrations of incompatible elements; this led to some exotic models, for instance, the anatexis of oceanic crust in the presence of NaCl brines (Lassiter et al., 2002). We believe that these problems can be easily solved supposing a heterogeneous distribution of Cl, $K_2O$, $H_2O$, and other components in the plume mantle instead of the shallow assimilation of seawater components. We assume that such a heterogeneity occurs both on the scale of large domains of the plume mantle, which is responsible for the main correlation trend, and on a smaller scale. This was demonstrated on the basis of melt inclusions in such typical intraplate magmas as kimberlites strongly enriched in sodium chloride (Kamenetsky et al., 2004), general models of chlorine balance in subduction zones (Philippot et al., 1998), and chlorine isotope systematics in oceanic basalts (Magenheim et al., 1995). These pieces of evidence suggest that no less than 70% of chlorine of the altered oceanic crust are involved in deep mantle recycling. Because of this, we believe that the three distinguished types of basaltic magmas (I, II, and III) correspond to three types of plume mantle sources (M1, M2, and M3, respectively), and the compositional variations of these magmas (Fig. 5; Kovalenko et al., 2006b) reflect the heterogeneity of these sources.

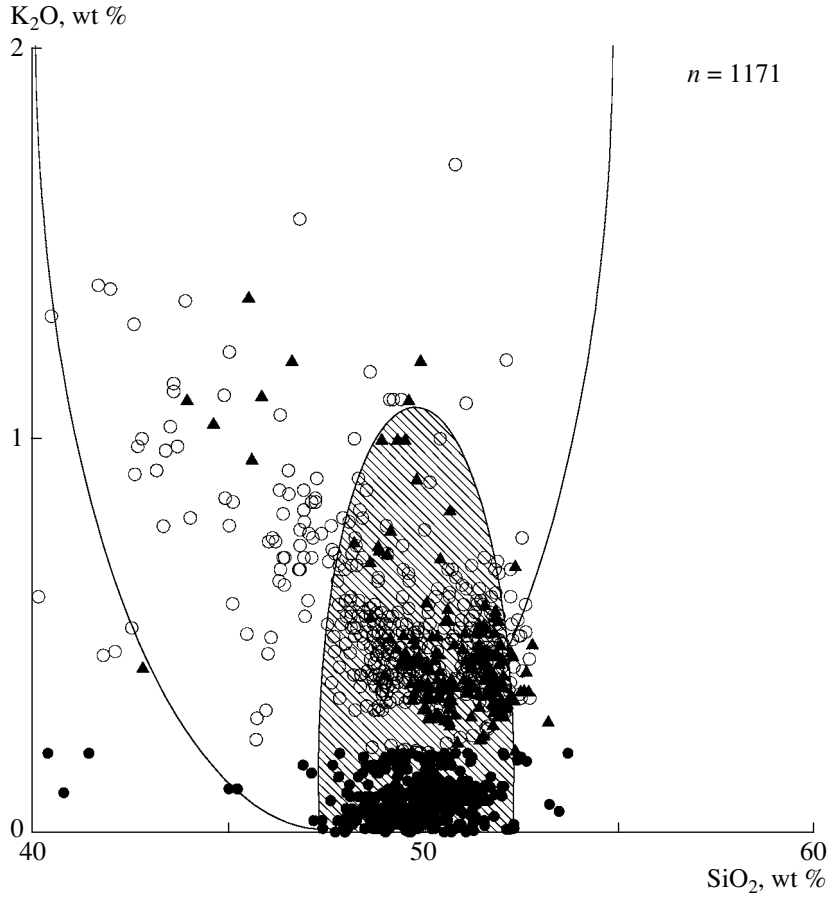


**Fig. 6.** Covariations of $SiO_2$ and $K_2O$ contents in the magmatic melts of ocean islands. Symbols are the same as in Fig. 5.

Let us estimate the average contents of volatile components and nonvolatile incompatible trace elements in these three sources of the plume mantle. To this end, we applied the same approach as for the average composition of the plume mantle. The model of thermal mantle plumes is based on the assumption that the concentrations of nonvolatile incompatible elements (at least potassium) in the plume mantle are identical to the respective characteristics of the DM (72 ppm $K_2O$). The following average concentrations of $H_2O$, Cl, and F were obtained for this model (Table 7): 130, 33, and 11 ppm for M1; 16, 1.7, and 9.2 ppm for M2; and 75, 4.1, and 6.8 ppm for M3. The average concentrations of nonvolatile incompatible trace elements estimated using this model are also shown in Table 7.

The second model implies that the average content of $K_2O$ in the M1 source is identical to that of DM (72 ppm), taking into account that the field of group I compositions practically coincides with the field of MOR magmas in Fig. 5. The average concentrations of $K_2O$ in mantle reservoirs M2 and M3 were taken to be equal to the average concentration in the OI mantle (510 ppm), although this value is probably underestimated because the compositions of field I were also used to obtain this estimate. Then, the average contents of $H_2O$, Cl, and F in the plume mantle will be the following (Table 5): 130, 33, and 11.3 ppm in M1; 110, 12, and 65 ppm in M2; and 530, 29, and 49 ppm in M3, with approximately equal degrees of melting in these three sources (0.09–0.12). The average concentrations of nonvolatile incompatible trace elements in mantle sources M1, M2, and M3 estimated for the model of a moderately enriched plume mantle are given in Table 7. The average sulfur contents estimated using Eq. (1) at $D = 0.114$ and $(1 - F) = 0.014$–$0.10$ (Table 3) for M1, M2, and M3 are, respectively, 110, 6.4, and 15.5 ppm for the thermal plume model and 110, 45, and 110 ppm for the model of an enriched reservoir (Table 7).

Figure 7 shows primitive mantle-normalized distribution patterns for trace elements, potassium, and volatile components in mantle reservoirs M1, M2, and M3 estimated using the models of thermal plumes (Fig. 7a) and enriched plume material (Fig. 7b). For the former model, the general level of normalized element concentrations in the plume mantle is lower than that in the primitive mantle, and the composition of M1 is similar to that of DM, except for the much higher Cl content. The composition of mantle reservoir M2 is more contrasting compared with M1 owing to the existence of pronounced negative anomalies of Cl, $H_2O$, and S.

**Table 5.** Average concentrations of major, volatile, and trace elements in three types of magmatic melts from ocean islands

| Component | Type I ($K_2O < 0.2$ wt %) | | | Type II ($K_2O > 0.2$ wt % and $H_2O < 0.2$ wt %) | | | Type III ($K_2O > 0.2$ wt % and $H_2O > 0.2$ wt %) | | |
|---|---|---|---|---|---|---|---|---|---|
| | *n* | arithm | geom | *n* | arithm | geom | *n* | arithm | geom |
| $SiO_2$ | 465 | 49.73 | 49.72 | 188 | 50.86 | 50.85 | 518 | 49.93 | 49.89 |
| | | 1.24 | 1.27–1.88 | | 1.41 | 1.44–1.39 | | 2.18 | 2.27–2.17 |
| $TiO_2$ | 451 | 0.92 | 0.96 | 184 | 2.44 | 2.46 | 512 | 2.59 | 2.60 |
| | | 0.54 | 0.59–0.36 | | 0.57 | 0.63–0.51 | | 0.41 | 0.46–0.40 |
| $Al_2O_3$ | 453 | 15.28 | 15.25 | 184 | 13.27 | 13.27 | 512 | 13.53 | 13.60 |
| | | 1.78 | 2.10–1.85 | | 0.82 | 0.84–0.79 | | 1.21 | 1.12–1.03 |
| FeO | 453 | 9.03 | 8.99 | 188 | 11.00 | 11.00 | 518 | 11.17 | 11.02 |
| | | 2.45 | 2.48–1.94 | | 0.71 | 0.71–0.67 | | 1.15 | 1.55–1.36 |
| MnO | 347 | 0.16 | 0.16 | 133 | 0.14 | 0.14 | 305 | 0.17 | 0.17 |
| | | 0.05 | 0.07–0.05 | | 0.06 | 0.06–0.04 | | 0.03 | 0.03–0.03 |
| MgO | 465 | 8.53 | 8.50 | 188 | 8.31 | 8.14 | 518 | 7.20 | 7.22 |
| | | 1.76 | 1.96–1.60 | | 2.97 | 3.40–2.40 | | 1.79 | 2.08–1.62 |
| CaO | 453 | 13.22 | 13.21 | 184 | 10.67 | 10.69 | 512 | 10.92 | 10.87 |
| | | 1.66 | 1.96–1.71 | | 1.09 | 1.14–1.03 | | 1.15 | 1.33–1.18 |
| $Na_2O$ | 451 | 1.96 | 1.92 | 184 | 2.33 | 2.33 | 512 | 2.44 | 2.44 |
| | | 0.46 | 0.50–0.40 | | 0.24 | 0.23–0.21 | | 0.54 | 0.49–0.41 |
| $K_2O$ | 465 | 0.07 | 0.07 | 188 | 0.41 | 0.40 | 518 | 0.53 | 0.53 |
| | | 0.06 | 0.11–0.04 | | 0.15 | 0.12–0.09 | | 0.28 | 0.23–0.16 |
| $P_2O_5$ | 359 | 0.09 | 0.08 | 180 | 0.26 | 0.25 | 470 | 0.27 | 0.27 |
| | | 0.08 | 0.10–0.04 | | 0.07 | 0.08–0.06 | | 0.09 | 0.10–0.07 |
| $H_2O$ | 81 | 0.24 | 0.24 | 188 | 0.10 | 0.10 | 518 | 0.55 | 0.62 |
| | | 0.11 | 0.11–0.08 | | 0.03 | 0.04–0.03 | | 0.29 | 0.30–0.20 |
| Cl | 140 | 280 | 290 | 106 | 90 | 90 | 280 | 320 | 310 |
| | | 480 | 2470–260 | | 70 | 80–40 | | 280 | 360–170 |
| F | 15 | 230 | 190 | 104 | 450 | 470 | 145 | 450 | 410 |
| | | 210 | 260–110 | | 220 | 200–150 | | 530 | 860–280 |
| S | 106 | 1090 | 1060 | 179 | 370 | 340 | 412 | 1130 | 1120 |
| | | 460 | 620–400 | | 340 | 520–200 | | 460 | 590–380 |
| $CO_2$ | 66 | 170 | 100 | 113 | 100 | 50 | 385 | 210 | 120 |
| | | 280 | 200–60 | | 170 | 180–40 | | 370 | 420–90 |
| Total | | 99.44 | 99.26 | | 99.89 | 99.74 | | 99.52 | 99.42 |
| Li | 9 | 3.82 | 3.81 | – | – | – | 11 | 4.08 | 4.07 |
| | | 0.46 | 0.48–0.43 | | – | – | | 0.37 | 0.39–0.36 |
| Be | 9 | 0.15 | 0.13 | – | – | – | 46 | 0.83 | 0.85 |
| | | 0.15 | 0.31–0.09 | | – | – | | 0.20 | 0.15–0.13 |
| B | 30 | 0.52 | 0.58 | – | – | – | 36 | 1.78 | 1.78 |
| | | 0.28 | 0.40–0.24 | | – | – | | 0.63 | 0.62–0.46 |
| Sc | 20 | 52.8 | 52.7 | – | – | – | 21 | 32.5 | 32.4 |
| | | 4.3 | 4.5–4.2 | | – | – | | 2.8 | 2.9–2.6 |
| V | 122 | 230 | 235 | 14 | 306 | 309 | 22 | 282 | 286 |
| | | 114 | 150–93 | | 42 | 39–35 | | 114 | 180–110 |
| Cr | 156 | 397 | 313 | 6 | 302 | 299 | 71 | 435 | 308 |
| | | 502 | 380–170 | | 132 | 203–121 | | 678 | 330–159 |
| Co | 21 | 51.8 | 52.3 | – | – | – | – | – | – |
| | | 7.5 | 10.4–8.7 | | – | – | | – | – |
| Ni | 22 | 79.9 | 78.1 | 112 | 195 | 205 | 37 | 326 | 349 |
| | | 26.0 | 28.2–20.7 | | 129 | 128–79 | | 138 | 205–129 |

**Table 5.** (Contd.)

| Component | Type I ($K_2O < 0.2$ wt %) | | | Type II ($K_2O > 0.2$ wt % and $H_2O < 0.2$ wt %) | | | Type III ($K_2O > 0.2$ wt % and $H_2O > 0.2$ wt %) | | |
|---|---|---|---|---|---|---|---|---|---|
| | *n* | arithm | geom | *n* | arithm | geom | *n* | arithm | geom |
| Rb | 18 | 0.76 | 0.67 | 7 | 6.52 | 6.48 | 53 | 10.9 | 10.5 |
| | | 0.72 | 0.26–0.19 | | 1.12 | 1.24–1.04 | | 5.9 | 5.8–3.7 |
| Sr | 146 | 100 | 101 | 14 | 529 | 484 | 60 | 439 | 442 |
| | | 52 | 57–36 | | 316 | 424–226 | | 205 | 290–175 |
| Y | 145 | 14.3 | 14.3 | 14 | 30.2 | 30.4 | 60 | 25.9 | 25.2 |
| | | 9.0 | 11.4–6.3 | | 5.9 | 6.1–5.1 | | 8.4 | 9.7–7.0 |
| Zr | 146 | 31.9 | 33.4 | 14 | 266 | 248 | 60 | 144 | 149 |
| | | 32.6 | 60.4–21.5 | | 188 | 280–132 | | 71 | 72–49 |
| Nb | 67 | 2.51 | 1.70 | 14 | 31.8 | 29.4 | 59 | 17.6 | 16.8 |
| | | 2.65 | 2.65–1.04 | | 29.4 | 58–19.5 | | 10.1 | 8.5–5.6 |
| Ba | 89 | 15.9 | 12.5 | 14 | 173 | 145 | 59 | 129 | 131 |
| | | 18.8 | 30.7–8.9 | | 141 | 215–87 | | 60 | 61–42 |
| La | 158 | 2.07 | 1.47 | 14 | 27.7 | 22.3 | 68 | 18.5 | 15.3 |
| | | 1.85 | 1.63–0.77 | | 24.6 | 39.1–14.2 | | 19.2 | 15.3–7.66 |
| Ce | 141 | 5.15 | 4.76 | 14 | 66.5 | 54.6 | 68 | 41.9 | 36.9 |
| | | 4.46 | 5.49–2.55 | | 56 | 89–34 | | 35.6 | 31.9–17.1 |
| Pr | 16 | 1.29 | 1.29 | – | – | – | 27 | 4.82 | 4.82 |
| | | 0.08 | 0.08–0.08 | | – | – | | 0.81 | 0.95–0.79 |
| Nd | 141 | 4.89 | 4.72 | 14 | 43.4 | 39.9 | 68 | 22.9 | 22.0 |
| | | 3.76 | 5.17–2.47 | | 31.3 | 49.2–22.0 | | 13.4 | 13.6–8.4 |
| Sm | 157 | 1.86 | 1.61 | 14 | 8.43 | 8.58 | 68 | 5.70 | 5.64 |
| | | 1.39 | 1.47–0.77 | | 4.56 | 6.25–3.62 | | 2.68 | 3.11–2.00 |
| Eu | 141 | 0.75 | 0.67 | 14 | 2.28 | 2.23 | 59 | 2.07 | 2.07 |
| | | 0.51 | 0.43–0.26 | | 0.69 | 0.75–0.56 | | 0.40 | 0.41–0.34 |
| Gd | 36 | 4.57 | 4.67 | 7 | 5.85 | 5.83 | 52 | 6.30 | 6.17 |
| | | 2.91 | 3.83–2.10 | | 0.60 | 0.62–0.56 | | 1.49 | 1.54–1.23 |
| Tb | 16 | 0.77 | 0.77 | – | – | – | 17 | 1.06 | 1.00 |
| | | 0.06 | 0.06–0.06 | | – | – | | 0.22 | 0.20–0.17 |
| Dy | 141 | 3.01 | 2.83 | 14 | 6.13 | 6.24 | 67 | 5.02 | 5.20 |
| | | 2.01 | 2.43–1.31 | | 1.30 | 1.65–1.31 | | 1.66 | 1.87–1.38 |
| Ho | 16 | 1.12 | 1.12 | – | – | – | 27 | 1.09 | 1.06 |
| | | 0.07 | 0.07–0.08 | | – | – | | 0.18 | 0.14–0.12 |
| Er | 141 | 1.94 | 1.76 | 13 | 2.87 | 2.91 | 65 | 2.53 | 2.50 |
| | | 1.21 | 1.33–0.76 | | 0.59 | 0.71–0.57 | | 0.86 | 0.94–0.68 |
| Tm | 16 | 0.47 | 0.48 | – | – | – | 17 | 0.41 | 0.42 |
| | | 0.03 | 0.04–0.04 | | – | – | | 0.09 | 0.10–0.08 |
| Yb | 157 | 1.80 | 1.64 | 14 | 2.30 | 2.41 | 68 | 2.09 | 2.16 |
| | | 1.10 | 1.13–0.67 | | 0.30 | 0.53–0.43 | | 0.77 | 0.88–0.63 |
| Lu | 16 | 0.44 | 0.44 | 6 | 0.31 | 0.31 | 27 | 0.34 | 0.34 |
| | | 0.03 | 0.04–0.04 | | 0.02 | 0.02–0.02 | | 0.07 | 0.08–0.06 |
| Hf | 21 | 1.87 | 1.73 | 6 | 3.76 | 3.88 | 45 | 4.11 | 4.04 |
| | | 0.32 | 0.37–0.31 | | 0.53 | 0.37–0.33 | | 1.05 | 1.16–0.90 |
| Ta | 16 | 0.08 | 0.08 | – | – | – | 27 | 1.04 | 1.04 |
| | | 0.02 | 0.02–0.01 | | – | – | | 0.24 | 0.24–0.20 |
| Pb | 20 | 0.26 | 0.30 | 6 | 6.30 | 6.27 | 27 | 0.78 | 0.90 |
| | | 0.09 | 0.11–0.08 | | 0.93 | 1.03–0.88 | | 0.41 | 0.46–0.31 |
| Th | 27 | 0.08 | 0.08 | 6 | 0.79 | 0.79 | 27 | 0.98 | 1.02 |
| | | 0.04 | 0.05–0.03 | | 0.07 | 0.07–0.07 | | 0.20 | 0.22–0.18 |
| U | 20 | 0.02 | 0.02 | 6 | 0.25 | 0.26 | 27 | 0.30 | 0.29 |
| | | 0.02 | 0.04–0.01 | | 0.03 | 0.05–0.04 | | 0.07 | 0.08–0.06 |

**Table 6.** Ratios of the average concentrations of components in various types of magmatic melts of ocean islands

| Ratio | Type I | Type II | Type III |
|---|---|---|---|
| $H_2O/Cl$ | 15 ± 11 | 11 ± 7 | 21 ± 14 |
| $H_2O/F$ | 13 ± 6 | 2.1 ± 0.7 | 15 ± 10 |
| $H_2O/P_2O_5$ | 3.0 ± 2.1 | 0.4 ± 0.1 | 2.3 ± 0.8 |
| Cl/F | 0.8 ± 0.8 | 0.2 ± 0.1 | 0.7 ± 0.8 |
| $K_2O/H_2O$ | 0.3 ± 0.3 | 4.0 ± 1.1 | 0.9 ± 0.3 |
| $K_2O/Cl$ | 4.4 ± 4.3 | 44 ± 29 | 18 ± 12 |
| $K_2O/F$ | 3.7 ± 3.7 | 8.5 ± 2.5 | 13 ± 8 |
| $K_2O/P_2O_5$ | 0.9 ± 0.8 | 1.6 ± 0.4 | 2.0 ± 0.7 |
| $TiO_2/H_2O$ | 4.0 ± 1.9 | 25 ± 7 | 4.2 ± 1.3 |
| $TiO_2/Cl$ | 60 ± 36 | 270 ± 170 | 87 ± 55 |
| $TiO_2/F$ | 51 ± 25 | 52 ± 15 | 63 ± 37 |
| $TiO_2/K_2O$ | 14 ± 11 | 6.2 ± 1.5 | 4.9 ± 1.4 |
| $TiO_2/P_2O_5$ | 12 ± 7 | 9.8 ± 2.5 | 10 ± 2 |
| $P_2O_5/Cl$ | 5.0 ± 4.0 | 28 ± 18 | 9.0 ± 6.1 |
| $P_2O_5/F$ | 4.2 ± 3.2 | 5.3 ± 1.7 | 6.6 ± 4.2 |

There are also positive anomalies of Nb, La, Ce, and Ti. With respect to Cl, $H_2O$, and S contents, the composition of M3 is transitional between M1 and M2. In general, the trace element distribution pattern of M3 is similar to that of M2, but the former is somewhat less fractionated.

The spidergram patterns of the plume mantle reservoirs for the model of a moderately enriched source lie at higher normalized concentrations (Fig. 7b). The main geochemical features of M1, M2, and M3 sources are similar to those obtained for the thermal model: M1 is in general close to the DM, except for the higher Cl content; M2 shows the most contrasting distribution patterns with positive anomalies of Nb, La, Ce, and Ti and negative anomalies of Cl, $H_2O$, and S; and the composition of M3 is transitional between M1 and M2, except for the highest normalized Cl, $H_2O$, and S contents in the M3 reservoir. In all the compositions, $H_2O$ is strongly depleted relative to the neighboring elements, which is again contrary to the idea of wet plumes.

Thus, the available data indicate that the plume mantle is not uniform and its heterogeneity can be described by the existence of three main compositions, one of which (M1) is similar to the MOR mantle, and two other constituents (M2 and M3) are moderately enriched in K, Ti, P, F, and incompatible trace elements but depleted in Cl, $H_2O$, and sometimes S. The compositions of M2 and M3 have different $H_2O$, Cl, and S contents: M2 is much poorer in these components than M3.

Of course, the heterogeneity of the plume mantle is not limited to these three compositions. It is possible that, similar to the source of MOR magmas (Kovalenko et al., 2006a), M1 includes an ultradepleted component and a relatively enriched component, which may approach the most potassium- and water-rich composition of M3 (Fig. 5). Similarly, the compositions of M2 and M3 could also be produced by mixing between the most anhydrous composition with the maximum $K_2O/H_2O$ ratio and a water-rich component with low $K_2O/H_2O$.

## CHEMICAL STRUCTURE OF MANTLE PLUMES

Figure 8 shows the compositions of OI magmas in the $K_2O/H_2O$–$H_2O/Cl$ and $K_2O/TiO_2$–$H_2O/TiO_2$ diagrams, which were previously considered by Kovalenko et al. (2004) on the basis of a smaller analytical database. It can be seen that the compositions of group I have the lowest $K_2O/H_2O$ and $K_2O/TiO_2$ values, whereas the compositions of group II show high $K_2O/H_2O$ ratios. Group I melts fall in general within the field of MOR magmas, whereas the compositions of groups II and III approach the CR field. In the diagrams of other incompatible elements (Figs. 9–11), the melt compositions of these groups occupy similar but not identical positions. In Fig. 9 field I also coincides with the compositional field of MOR magmas. With respect to the $K_2O/TiO_2$ ratio, field II coincides with field III but deviate from it in the $K_2O/H_2O$ ratio extending even beyond the field of CR melts. This suggests that at least three components contributed to the source of OI magmas: ultradepleted mantle material (Kovalenko et al., 2006b) with the lowest $K_2O/TiO_2$ and $K_2O/H_2O$ ratios, enriched material with high $K_2O/TiO_2$ and low $K_2O/H_2O$ ratios, and enriched material with high $K_2O/TiO_2$ and $K_2O/H_2O$ ratios.

In the diagrams of various ratios with chlorine (Fig. 10), the compositions of field III are transitional between fields I and II. This suggests that mantle reservoir M3 is probably a product of mixing between M1 and M2 compositions. The compositions of M1 + M3 approach those of MOR magma sources, and M2 is close to the composition of the CR source. Each field shows a positive correlation between $H_2O/Cl$ and $K_2O/Cl$, which could have been explained by the assimilation of seawater components by the magmas. The composition of seawater has $H_2O/Cl \sim 50$ (Fig. 10a) and cannot be responsible for the above correlations. However, they could be related to the assimilation of brines with low $H_2O/Cl$ ratios formed by the unmixing of seawater. However, in such a case, it is difficult to explain the correlation of $H_2O/Cl$ with $TiO_2/H_2O$ (Fig. 10b). The logarithms of Cl/F and $H_2O/Cl$ ratios show a negative correlation (Fig. 10c). With respect to $H_2O/Cl$, fields I + III and II overlap, but field II lies in the region of low Cl/F values, corresponding to the lower average contents of Cl and $H_2O$ in these magmas. The correlations shown in Fig. 10c, as well as those of Figs. 10a and 10b, are adequately explained by the model of deep recycling of crustal materials.

**Table 7.** Average concentrations of elements (ppm) in the mantle plume sources of ocean islands calculated on the basis of two models

| Component | Type I | *n* | Type II | *n* | Type III | *n* |
|---|---|---|---|---|---|---|
| | | | Thermal model | | | |
| $K_2O$ | 72 | | 72 | | 72 | |
| $H_2O$ | 130 (+48/–35) | 81 | 16 (+10/–6) | 188 | 75 (+39/–25) | 518 |
| Cl | 33 (+118/–26) | 142 | 1.7 (+1.0/–0.6) | 106 | 4.1 (+4.0/–2.0) | 314 |
| F | 11 (+11/–6) | 15 | 9.2 (4.6/–3.1) | 104 | 6.8 (+12.1/–4.4) | 145 |
| S | 110 (+119/–57) | 108 | 6.4 (+12.3/–4.2) | 179 | 15.5 (+9.0/–5.7) | 412 |
| $TiO_2$ | 978 (+1000/–494) | 451 | 429 (+87/–72) | 184 | 378 (+137/–100) | 512 |
| $P_2O_5$ | 80 (+80/–39) | 359 | 46 (+13/–10) | 180 | 40 (+10/–8) | 470 |
| Sr | 12 (+17/–7) | 146 | 5.3 (+1.0/–0.8) | 14 | 4.2 (+3.4/–1.9) | 60 |
| Y | 2.1 (+3.2/–1.3) | 145 | 0.34 (+0.24/–0.14) | 14 | 0.32 (+0.22/–0.13) | 60 |
| Zr | 4.5 (+5.5/–2.5) | 146 | 2.9 (+0.4/–0.4) | 14 | 1.8 (+1.5/–0.8) | 60 |
| Nb | 0.17 (+0.08/–0.05) | 67 | 0.31 (+0.14/–0.10) | 14 | 0.25 (+0.13/–0.08) | 50 |
| Ba | 1.4 (+0.9/–0.6) | 89 | 1.6 (+0.3/–0.2) | 14 | 1.7 (+0.4/–0.3) | 50 |
| La | 0.23 (+0.19/–0.10) | 158 | 0.39 (+0.08/–0.06) | 14 | 0.19 (+0.21/–0.10) | 68 |
| Ce | 0.66 (+0.48/–0.28) | 141 | 0.57 (+0.16/–0.12) | 14 | 0.45 (+0.37/–0.20) | 68 |
| Nd | 0.62 (+0.70/–0.33) | 141 | 0.40 (+0.09/–0.07) | 14 | 0.29 (+0.20/–0.12) | 68 |
| Sm | 0.22 (+0.36/–0.14) | 157 | 0.09 (+0.02/–0.02) | 14 | 0.07 (+0.06/–0.03) | 68 |
| Eu | 0.08 (+0.13/–0.05) | 141 | 0.02 (+0.02/–0.01) | 14 | 0.02 (+0.01/–0.01) | 50 |
| Dy | 0.36 (+0.69/–0.23) | 141 | 0.07 (+0.05/–0.03) | 14 | 0.05 (+0.06/–0.03) | 67 |
| Yb | 0.23 (+0.48/–0.15) | 157 | 0.02 (+0.02/–0.01) | 14 | 0.02 (+0.02/–0.01) | 68 |
| | | | Enriched source model | | | |
| $K_2O$ | 72 | | 510 | | 510 | |
| $H_2O$ | 130 (+48/–35) | 81 | 110 (+70/–40) | 188 | 530 (+280/–180) | 518 |
| Cl | 33 (+118/–26) | 142 | 12 (+7/–4) | 106 | 29 (+28/–14) | 314 |
| F | 11 (+11/–6) | 15 | 65 (+33/–22) | 104 | 49 (+86/–31) | 145 |
| S | 110 (+119/–57) | 108 | 45 (+87/–30) | 179 | 110 (+65/–41) | 412 |
| $TiO_2$ | 978 (+1000/–494) | 451 | 3000 (+660/–540) | 184 | 2700 (+990/–720) | 512 |
| $P_2O_5$ | 80 (+80/–39) | 359 | 330 (+90/–70) | 180 | 280 (+75 /–60) | 470 |
| Sr | 12 (+17/–7) | 146 | 38 (+7/–6) | 14 | 30 (+24/–13) | 60 |
| Y | 2.1 (+3.2/–1.3) | 145 | 2.4 (+1.7/–1.0) | 14 | 2.2 (+1.6/–0.9) | 60 |
| Zr | 4.5 (+5.5/–2.5) | 146 | 20 (+3/–3) | 14 | 13 (+10/–6) | 60 |
| Nb | 0.17 (+0.08/–0.05) | 67 | 2.2 (+1.0/–0.7) | 14 | 1.8 (+0.9/–0.6) | 50 |
| Ba | 1.4 (+0.9/–0.6) | 89 | 11 (+2/–2) | 14 | 12 (+3/–2) | 50 |
| La | 0.23 (+0.19/–0.10) | 158 | 1.7 (+0.6/–0.4) | 14 | 1.3 (+1.5/–0.7) | 68 |
| Ce | 0.66 (+0.48/–0.28) | 141 | 4.0 (+1.1/–0.9) | 14 | 3.2 (+2.7/–1.4) | 68 |
| Nd | 0.62 (+0.70/–0.33) | 141 | 2.8 (+0.6/–0.5) | 14 | 2.0 (+1.4/–0.8) | 68 |
| Sm | 0.22 (+0.36/–0.14) | 157 | 0.66 (+0.14/–0.12) | 14 | 0.48 (+0.46/–0.23) | 68 |
| Eu | 0.08 (+0.13/–0.05) | 141 | 0.17 (+0.11/–0.07) | 14 | 0.16 (+0.05/–0.04) | 50 |
| Dy | 0.36 (+0.69/–0.23) | 141 | 0.51 (+0.36/–0.21) | 14 | 0.37 (+0.45/–0.20) | 67 |
| Yb | 0.23 (+0.48/–0.15) | 157 | 0.16 (+0.15/–0.08) | 14 | 0.12 (+0.13/–0.06) | 68 |

Note: *n* is the number of determinations. Numbers in parentheses show the deviations from the average values.

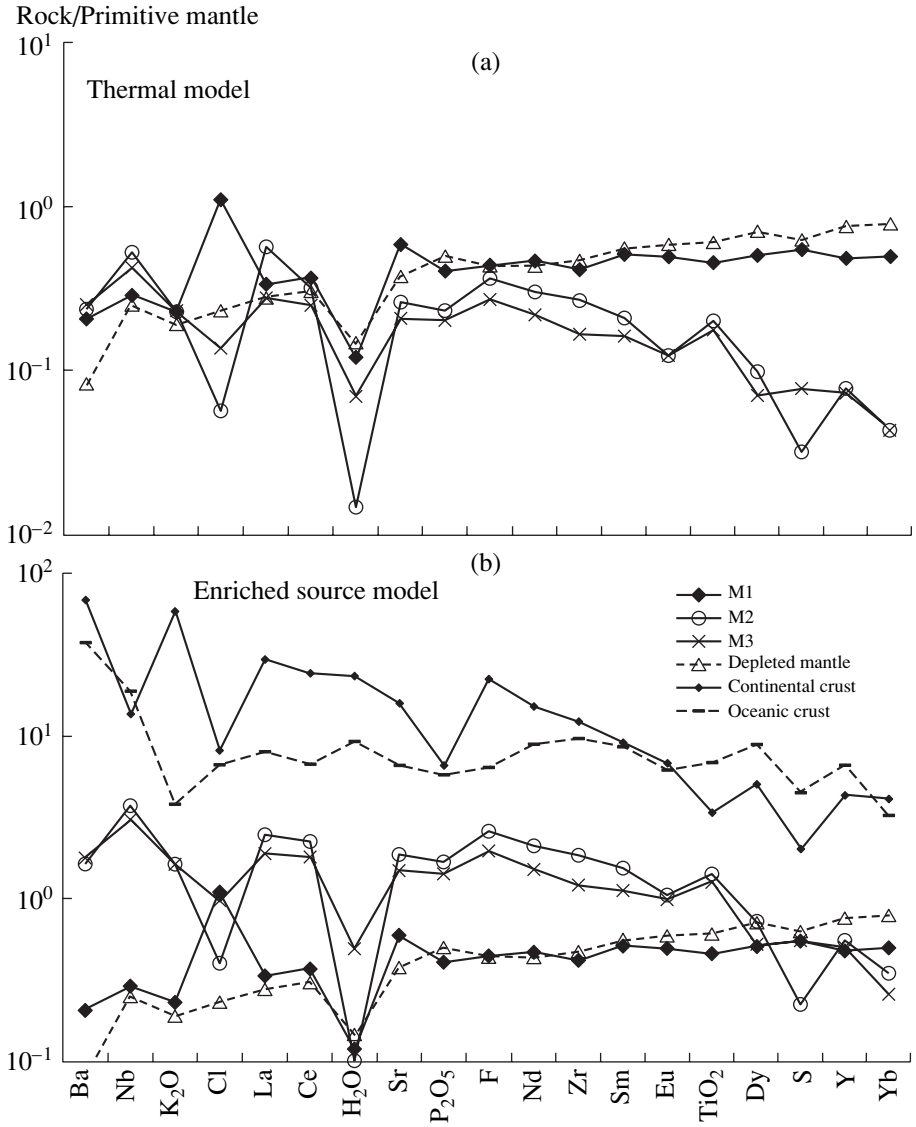


**Fig. 7.** Spider diagrams for trace elements and volatile components in mantle reservoirs M1, M2, and M3 estimated on the basis of (a) the thermal model and (b) the model of an enriched source. Also shown are the compositions of the depleted mantle (source of mid-ocean ridge basalts) after Workman and Hart (2005), continental crust (Rudnick and Gao, 2003), and oceanic crust (Ronov et al., 1990); the composition of the primitive mantle is after Palme and O'Neill (2003).

The compositions of fields I and III display negative correlations in the $TiO_2/H_2O$–$K_2O/TiO_2$ diagram (Fig. 11a) and positive correlations in the $K_2O/TiO_2$–$K_2O/F$ diagram (Fig. 11b). The compositions of group II deviate toward more anhydrous compositions in Fig. 11a and overlap fields I and III in Fig. 11b. A notable feature of the diagram in Fig. 11b is the presence of a number of compositions with high $K_2O/F$ ratios. It can be supposed that the plume mantle of field M3 includes a component with high $K_2O/F$ (depleted in F). Such compositions (20–110 ppm F) were reported in a single publication (Garcia et al., 1989) for the submarine tholeiitic glasses of the Hawaii, but the reliability of these results is supported by the high sensitivity of F analysis (1 ppm).

The data shown in Figs. 8–11 suggest that the plume mantle is formed by mixing ultradepleted, enriched anhydrous, and enriched hydrated materials. It is also noteworthy that the dry component (M2) is similar to the isotopic component EM, which probably has a low $H_2O/Ce$ ratio (Dixon et al., 2002). The composition of the EM reservoir plots at low $H_2O/K_2O$ ratios (Fig. 5). The data of Dixon et al. (2002) show that the compositions involving the EM isotopic component are characterized by a positive correlation between $K_2O$ and $H_2O$: $\log K_2O = 1.521 \log H_2O - 0.064$, $R^2 = 0.53$, and the compositions connected with the isotopic component FOZO are approximated by the expression $\log K_2O = 0.864 \log H_2O$, $R^2 = 0.86$. At a given $K_2O$ concentra-

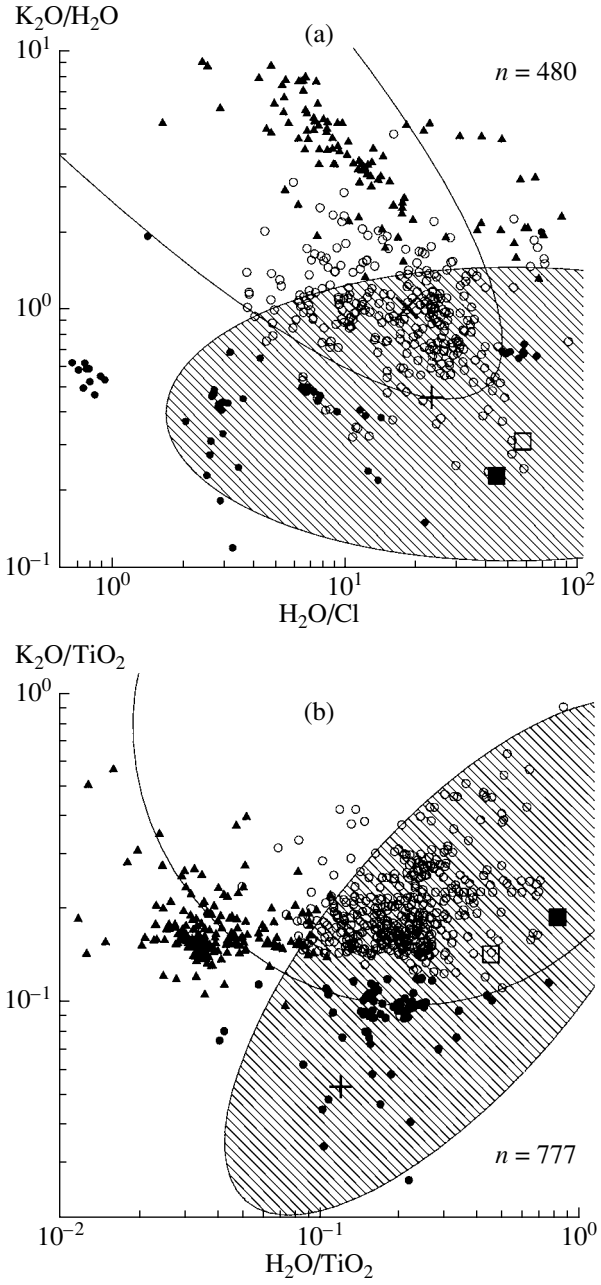


**Fig. 8.** Diagrams of (a) $K_2O/H_2O$–$H_2O/Cl$ and (b) $K_2O/TiO_2$–$H_2O/TiO_2$ for the magmatic melts of ocean islands. Symbols are the same as in Fig. 5.

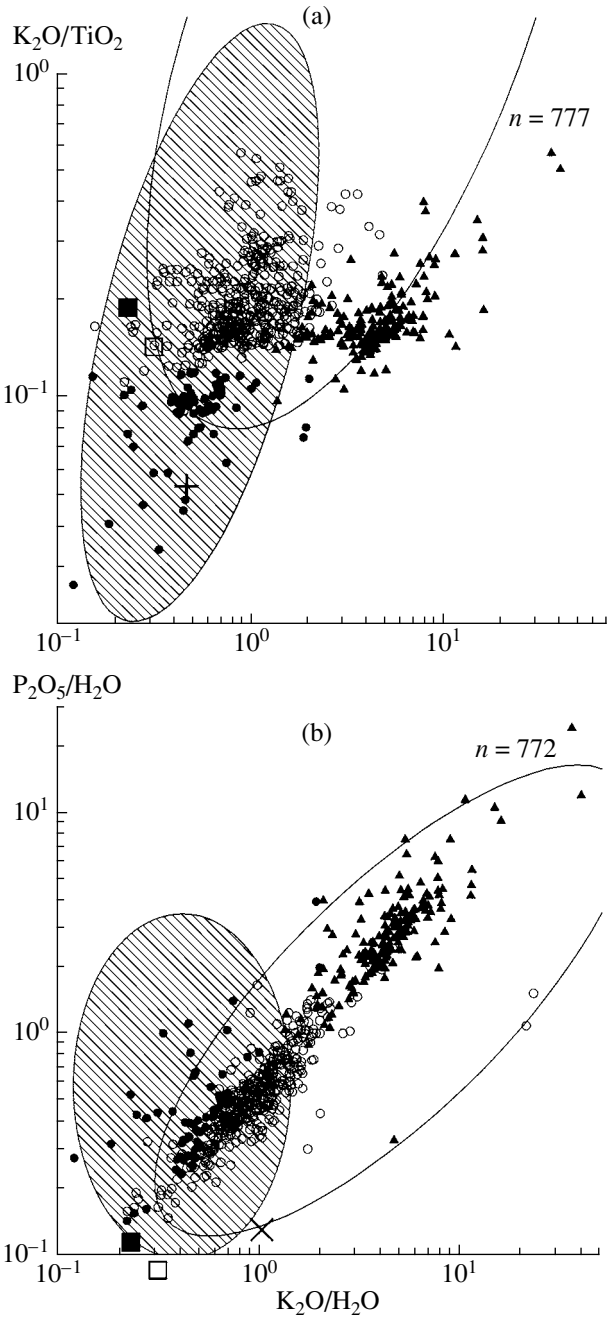


**Fig. 9.** Diagrams of (a) $K_2O/TiO_2$–$K_2O/H_2O$ and (b) $P_2O_5/H_2O$–$K_2O/H_2O$ for the magmatic melts of ocean islands. Symbols are the same as in Fig. 5.

tion, the content of $H_2O$ calculated by the latter equation is higher, i.e., the compositions with EM isotopic signatures are dryer and tend to plot closer to field II. Thus, high $H_2O/K_2O$ ratios are characteristic of both the DM and the plume sources of the HIMU and FOZO isotopic types. In addition to the three main components, the plume mantle may include components enriched in Cl and depleted in F. In our opinion, they are entrained into the plume mantle through the recycling of components of the oceanic and continental crust. Let us consider the possible mechanisms of mixing of three main components, M1, M2, and M3 in the plume mantle.

All the described features in the behavior of incompatible elements in the basic magmas of OI (Figs. 5, 8–11) can be explained by the model of a zoned mantle plume, which was proposed for the Hawaiian Islands (Sen et al., 1996) (Fig. 12). It is assumed that the mantle plume ascends to the lithosphere–asthenosphere boundary. The material of the plume itself produces OI

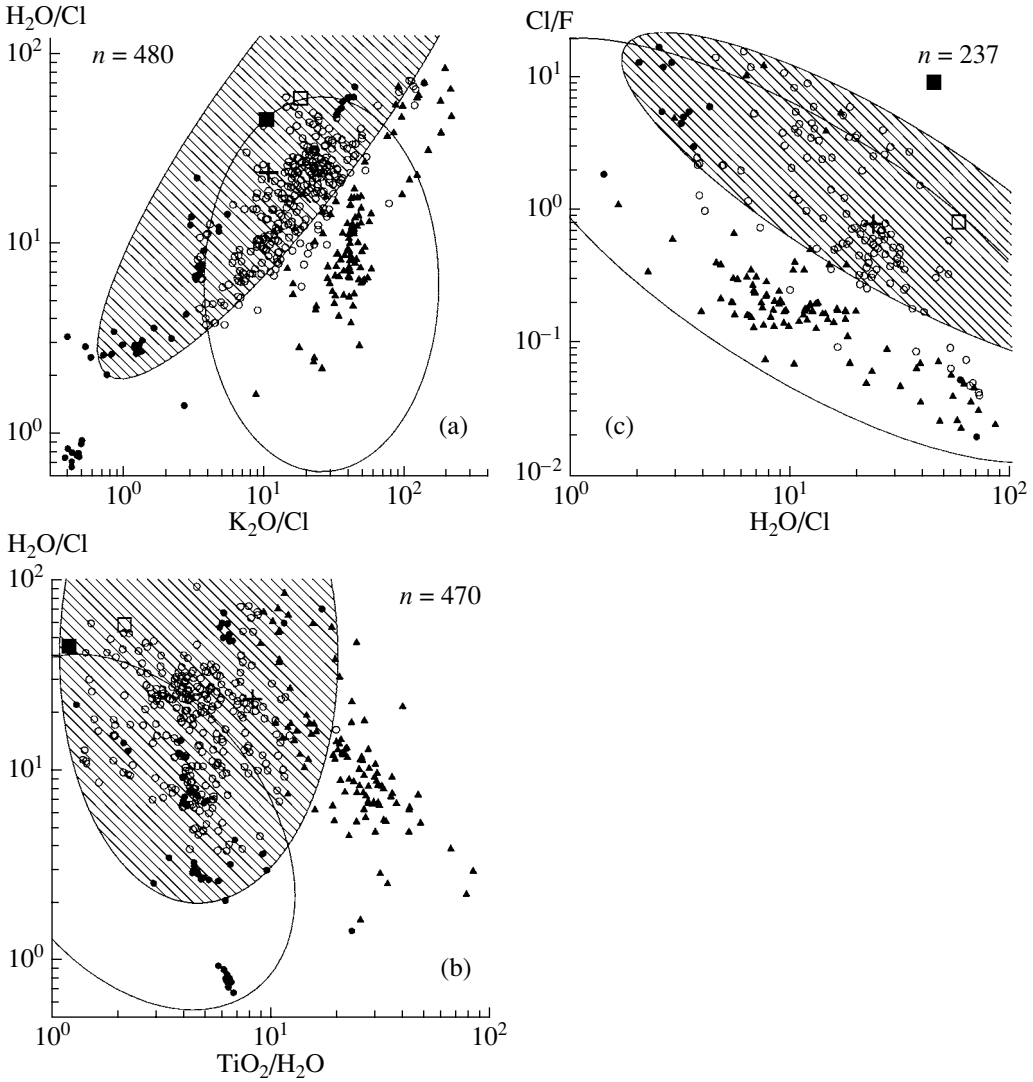


**Fig. 10.** Diagrams of (a) $H_2O/Cl–K_2O/Cl$, (b) $H_2O/Cl–TiO_2/H_2O$, and (c) $Cl/F–H_2O/Cl$ for the magmatic melts of ocean islands. Symbols are the same as in Fig. 5.

magmas of fields II and III. The compositions of field II could be formed in the central hotter parts of the plume at the maximum degrees of melting, which resulted in the formation of the most anhydrous magmas. The compositions of field III could be derived from the outer parts of the mantle plume, which must be colder and richer in water, chlorine, and sulfur compared with the M2 composition (Table 5). With respect to other components, the plume magmas of fields II and III are similar to each other but different from field I magmas in higher $K_2O$, $TiO_2$, $P_2O_5$, and other incompatible element contents. Since the compositions of field I are similar in all respects to MOR magmas, it is suggested that they are generated in the zone of interaction between the plume and the enclosing depleted mantle. According to physical models of mantle plumes (Hauri et al., 1994), the enclosing depleted mantle must be entrained along the plume boundary from great depths. This implies that depleted mantle material occurs at greater depths than the depth of melt generation. Correspondingly, the magmas of field III are derived from a mixture of the plume and depleted mantle components. The fraction of the former component increases toward the center of the plume, which results in the formation of a continuous series of field I compositions (Figs. 5–11) from MOR-type magmas and even more depleted compositions to field III magmas. Such a model explains the gap between fields I and II (Fig. 5) by the low probability of a direct contact and interaction between the hot plume core and the enclosing depleted mantle. The simple model of the formation of field III magmas by mixing of field I and II compositions is disturbed for $H_2O$, Cl, and S, i.e., the volatile components that are most likely redistributed between the plume and enclosing mantle. It is possible that this concerns also some nonvolatile incompatible elements (Table 5).

The homogenization temperatures of melt inclusions provide no evidence for the higher temperatures of the dry and chlorine- and sulfur-poor magmas of field II compared with field I melts. However, the entrapment temperatures of melt inclusion reflect the conditions of phenocryst crystallization in magma chambers and conduits, and these data do not therefore contradict the suggestion of high temperatures in the central parts of plumes. The depletion of $H_2O$, Cl, and S in the central parts of plumes may reflect some compositional peculiarities of the primary matter of these zones (Sobolev et al., 2005). According to some recent data, the recycled lithosphere entrained into mantle plumes must be strongly (up to 95%) dehydrated (Dixon et al., 2002). Our data (Table 5) show that, if the composition of such lithosphere corresponds to an M2-type source, its water content is slightly lower than that of the depleted mantle (Kovalenko et al., 2006b; Salters and Stracke, 2004). It is reasonable to suppose that even if the recycled lithosphere was severely dehydrated during subduction, its material could not remain absolutely anhydrous owing to the migration of water from the surrounding water richer mantle material. The Cl content of M2 is higher than that of the DM, which is in agreement with the smaller loss of Cl compared with water during lithosphere subduction. The M2 composition is depleted in S compared with the DM, but the behavior of S in rocks during subduction is not fully understood. It can be supposed that the abundance of S in M2 decreases owing to the high oxygen fugacity in the recycled lithosphere, which increases the solubility of S in fluids. However, the content of S in M3 is as high as in the DM.

Thus, the model considered here suggests a mixed nature of a mantle plume in the geodynamic environment of OI. We favor the moderately enriched average composition of the plume mantle. Furthermore, plumes may probably be zoned: their central parts are moderately enriched in nonvolatile incompatible elements but depleted in $H_2O$, Cl, and S; whereas the moderately enriched periphery has also high contents of these volatile components. The DM surrounding plumes is also enriched in $H_2O$, Cl, and F compared with the DM not affected by plumes.

A comparison of the compositions of M1, M2, and M3 sources with model reservoirs [primitive mantle after Palme and O'Neill (2003); depleted mantle after Salters and Stracke (2004) with $H_2O$, Cl, F, and S after Kovalenko et al. (2006b); continental crust after Rudnick and Gao (2003); and oceanic crust after Ronov et al. (1990)] shows (Figs. 8–11) that the compositions of field III and I magmas are well approximated by mixing between the compositions of DM and continental crust. This supports the participation of the continental crust or its components in mantle recycling, which was supposed by many authors. In accordance with the proposed model (Fig. 12), this happens at the contact of the plume with the enclosing mantle as a result of mixing between M1 and M3 materials (Figs. 8–11). It is possible that the derivatives of M3 and in part M1 are enriched in volatile and other incompatible elements at the expense of the "suction" of the deep enclosing mantle along the plume boundary (Hauri et al., 1994).

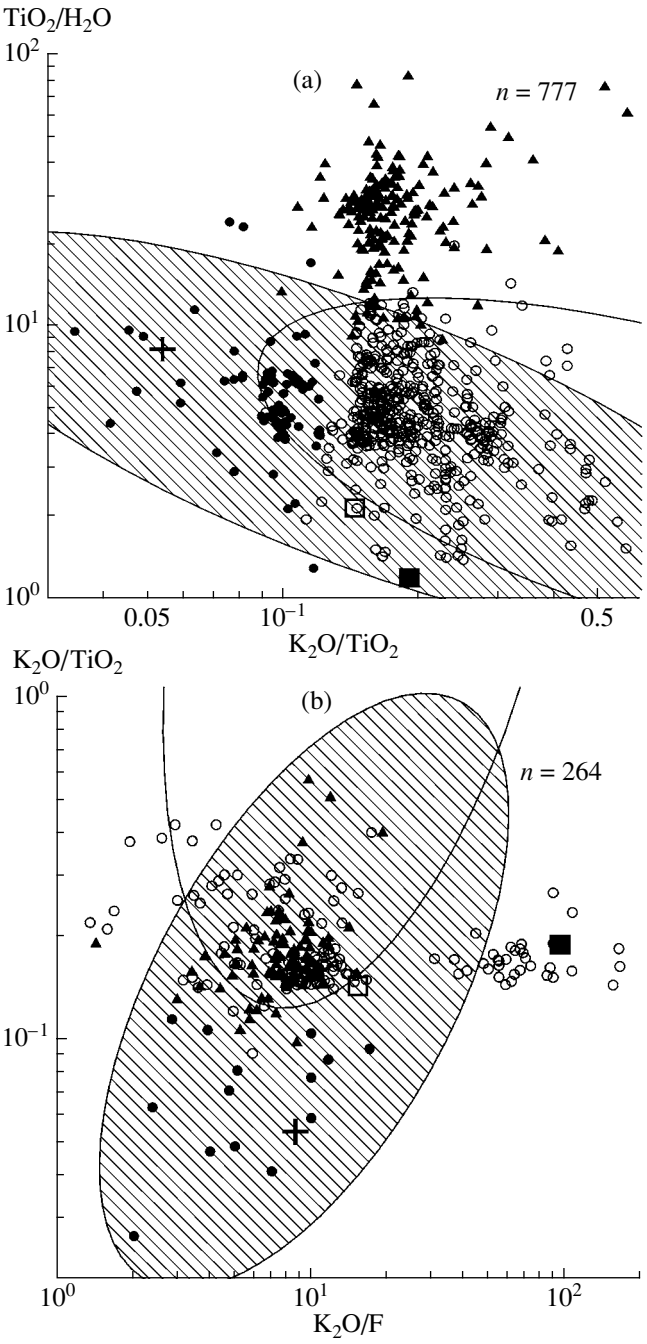


**Fig. 11.** Diagrams of (a) $TiO_2/H_2O$–$K_2O/TiO_2$ and (b) $K_2O/TiO_2$–$K_2O/F$ for the magmatic melts of ocean islands. Symbols are the same as in Fig. 5.

The described generalized model is based on the compositions of magmas from all known modern or young plumes responsible for ocean island magmatism. In this connection, a question arises as to the validity of

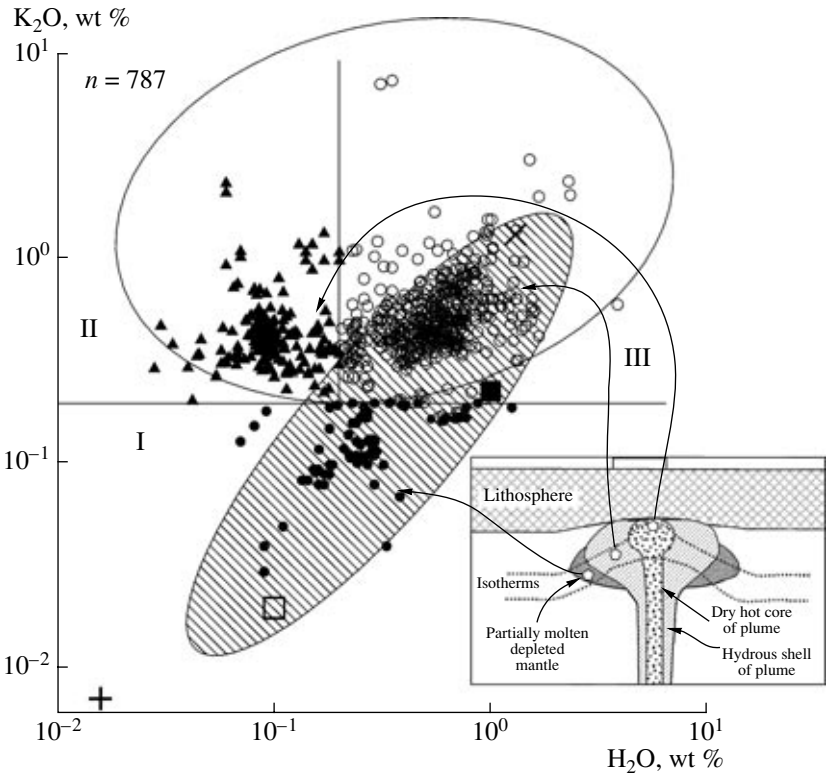


**Fig. 12.** Generalized model for the compositional structure of a mantle plume beneath ocean islands. Symbols are the same as in Fig. 5.

this model for particular complexes (Table 8). The model is evidently valid for the Hawaiian plume, which is represented by the maximum number of magma compositions corresponding to all the three sources (Dixon and Clague, 2001 and references therein). According to Dixon and Clague (2001), the central hot part of the plume (KOO and KEA isotopic reservoirs) is depleted in water but enriched in nonvolatile incompatible trace elements (M2), the periphery of the plume core is hot, contains a considerable fraction of lower mantle material (FOZO component), and is compositionally similar to M3; and the peripheral zone of the plume is characterized by interaction with the enclosing asthenosphere (M1). Much less data are available for other plumes (Table 8). For instance, the plume of the Ontong–Java plateau is represented by 77 magma compositions of group I and only five compositions of group III. Almost all the available compositions for the Reunion plume (52 from 53) belong to group III. It is not yet clear whether this is related to the insufficient amount of analytical data or to the predominance of one of the three sources in particular plumes.

**Table 8.** Number of analyses of melt inclusions and quenched glasses representing three types of magmatic melts from various complexes of oceanic islands and plateaus

| Location | Type of magmatic melt | | |
|---|---|---|---|
| | I | II | III |
| Iceland | 218 | 31 | 49 |
| Ontong–Java Plateau | 77 | – | 5 |
| Galapagos Islands | 74 | – | – |
| Hawaii | 40 | 425 | 681 |
| Kerguelen | 18 | - | 44 |
| Canary Islands | – | 154 | 81 |
| Austral Islands | – | 3 | 18 |
| Reunion Island | – | 1 | 52 |

## CONCLUSIONS

(1) If a reasonable interval of 0.02–0.2 is accepted for the degree of mantle source melting, the difference between the ratios of highly incompatible elements (K, Ce, $H_2O$, Cl, F, P, Ti, and many other trace elements) in magmas and their sources is no higher than 10%, which is comparable with the analytical errors. This allows us to consider the ratios of these components in magmas as proxies for the corresponding values in the source.

(2) Using the average composition and incompatible element ratios of ocean island magmas, we calculated average concentrations of volatile and nonvolatile elements for the plume mantle. The following values were obtained for volatile components in the plume mantle:

520 ppm $H_2O$, 21 ppm Cl, 55 ppm F, and 83 ppm S, which are significantly higher than those of the depleted mantle, except for the lower S content in the plume mantle. The plume mantle can therefore be characterized as moderately enriched and similar to the primitive mantle. On the other hand, the abundance of water is low relative to the elements of similar incompatibility, which is contrary to the idea of wet mantle plumes.

(3) Three types of basalt magmas (I, II, and III) and three corresponding types of plume mantle sources (M1, M2, and M3) were distinguished. Based on the model of a moderately enriched source, the average contents of $H_2O$, Cl, F, and S in the plume reservoirs were estimated as 130, 33, 11.3, and 110 ppm for M1; 110, 12, 65, and 45 ppm for M2; and 530, 29, 49, and 110 ppm for M3.

(4) The M1 reservoir is enriched in Cl and depleted in S compared with the primitive mantle and is similar to the DM composition in terms of other elements. The M2 reservoir is characterized by more contrasting incompatible element patterns with positive anomalies at $K_2O$ and Nb and negative anomalies at Cl, $H_2O$, and S. The M3 reservoir is intermediate between the compositions of M1 and M2, except for the contents of Cl, $H_2O$, and S, which are the highest in M3.

(5) The plume mantle is not uniform, and its heterogeneity is related to the existence of three main compositions, one of which (M1) is similar to the MOR mantle and two others (M2 and M3) are moderately enriched in K, Ti, P, and F but depleted in Cl and $H_2O$. The composition of M2 is depleted in $H_2O$, Cl, and S and enriched in incompatible trace elements compared with that of M3.

(6) The formation of plume magmas involved three main sources: ultradepleted mantle, enriched dry mantle, and enriched hydrated mantle. The dry component (M2) is probably similar to the isotopic component EM. In addition to the three main components, the plume mantle may contain components enriched in Cl and depleted in F. They could be entrained into the plume mantle owing to the deep recycling of the components of the oceanic and continental crust.

(7) The established relationships are in agreement with the zonal model of a mantle plume, which includes a hot central part depleted in $H_2O$, Cl, and S and enriched in nonvolatile incompatible trace elements; a periphery enriched in volatile and nonvolatile elements; and the enclosing mantle interacting with the plume material.

## ACKNOWLEDGMENTS

This study was financially supported by the Russian Foundation for Basic Research (project nos. 04-05-65123, 05-05-64000, 05-05-64175, and 05-05-64056), Russian President's Program for the Support of Leading Scientific Schools (grant nos. NSh-1145.2003.5 and NSh-1618.2003.5), and Priority Research Program no. 5 of the Department of the Earth Sciences, Russian Academy of Sciences.

## REFERENCES

1. F. Brunet and G. Chazot, "Partitioning of Phosphorus between Olivine, Clinopyroxene and Silicate Glass in a Spinel Lherzolite Xenolith from Yemen," Chem. Geol. **176**, 51–72 (2001).
2. J. E. Dixon and D. A. Clague, "Volatiles in Basaltic Glasses from Loihi Seamount, Hawaii: Evidence for a Relatively Dry Plume Component," J. Petrol. **42**, 627–654 (2001).
3. J. E. Dixon, E. M. Stolper, and J. R. Delaney, "Infrared Spectroscopic Measurements of $CO_2$ and $H_2O$ Glasses in the Juan De Fuca Ridge Basaltic Glasses," Earth Planet. Sci. Lett. **90**, 87–104 (1988).
4. J. E. Dixon, L. Leist, Ch. Langmuir, and J.-G. Schilling, "Recycled Dehydrated Lithosphere Observed in Plume-Influenced Mid-Oceanic-Ridge Basalts," Nature **420**, 385–389 (2002).
5. M. O. Garcia, D. W. Muenow, K. E. Aggrey, and J. R. O'Neil, "Major Element, Volatile, and Stable Isotope Geochemistry of Hawaiian Submarine Tholeiitic Glasses," J. Geophys. Res. **94**, 10525–10538 (1989).
6. D. H. Green, J. Falloon, S. M. Eggins, and G. M. Yaxley, "Primary Magmas and Mantle Temperatures," Eur. J. Mineral. **13**, 437–451 (2001).
7. E. Hauri, "SIMS Analysis of Volatiles in Silicate Glasses, 2: Isotopes and Abundances in Hawaiian Melt Inclusions," Chem. Geol. **183**, 115–141 (2002).
8. E. H. Hauri, J. A. Whitehead, and S. R. Hart, "Fluid Dynamic and Geochemical Aspects of Entrainment in Mantle Plumes," J. Geophys. Res. **99**, 24275–24300 (1994).
9. G. Hirth and D. L. Kohlstedt, "Water in the Oceanic Upper Mantle: Implications for Rheology, Melt Extraction and the Evolution of the Lithosphere," Earth Planet. Sci. Lett. **144**, 93–108 (1996).
10. A. W. Hofmann, "Mantle Geochemistry: The Message from Oceanic Volcanism," Nature **385**, 219–229 (1997).
11. A. W. Hofmann, "Sampling Mantle Heterogeneity through Oceanic Basalts: Isotopes and Trace Elements," in *Treatise on Geochemistry* (Elsevier, Amsterdam, 2003), Vol. 2, pp. 61–101.
12. M. B. Kamenetsky, A. V. Sobolev, V. S. Kamenetsky, et al., "Kimberlite Melts Rich in Alkali Chlorides and Carbonates: A Potent Metasomatic Agent in the Mantle," Geology **32**, 845–848 (2004).
13. V. I. Kovalenko, V. B. Naumov, V. V. Yarmolyuk, et al., "Balance of $H_2O$ and Cl between the Earth's Mantle and Outer Shells," Geokhimiya, No. 10, 1041–1070 (2002) [Geochem. Int. **40**, 929–942 (2002)].
14. V. I. Kovalenko, A. V. Girnis, V. A. Dorofeeva, et al., "Magma Sources of Ocean Islands," Dokl. Akad. Nauk **398**, 379–384 (2004) [Dokl. Earth Sci. **398**, 995–1000 (2004)].
15. V. I. Kovalenko, V. B. Naumov, A. V. Girnis, et al., "Estimation of the Average Contents of $H_2O$, Cl, F, and S in the Depleted Mantle on the Basis of the Compositions of Melt Inclusions and Quenched Glasses of Mid-Ocean

Ridge Basalts," Geokhimiya, No. 3, 243–266 (2006a) [Geochem. Int. **44**, 209–231 (2006a)].

16. V. I. Kovalenko, V. B. Naumov, A. V. Girnis, et al., "Volatiles in the Basaltic Magmas and Mantle Sources of Oceanic Islands: I. Estimation of the Melt Composition on the Basis of the Composition of Melt Inclusions and Rock Glasses," Geokhimiya (2006b) (in press).
17. V. I. Kovalenko, V. B. Naumov, A. V. Girnis, et al., "Volatiles in the Basaltic Magmas and Mantle Sources of Oceanic Islands: II. Estimation of the Contents in Mantle Reservoirs," Geokhimiya (2006c) (in press).
18. J. C. Lassiter, E. H. Hauri, I. K. Nikogosian, and H. G. Barsczus, "Chlorine–Potassium Variations in Melt Inclusions from Raivavae and Rapa, Austral Islands: Constraints on Chlorine Recycling in the Mantle and Evidence for Brine-Induced Melting of Oceanic Crust," Earth Planet. Sci. Lett. **202**, 525–540 (2002).
19. S. Maaloe, "Estimation of the Degree of Partial Melting Using Concentration Ratios," Geochim. Cosmochim. Acta **58**, 2519–2525 (1994).
20. A. G. Magenheim, A. G. Spivack, P. J. Michael, and J. M. Gieskes, "Chlorine Stable Isotope Composition of the Oceanic Crust: Implication for the Earth's Distribution of Chlorine," Earth Planet. Sci. Lett. **131**, 427–432 (1995).
21. D. Massare, N. Metrich, and R. Clocchiatti, "High-Temperature Experiments on Silicate Melt Inclusions in Olivine at 1 atm: Inference on Temperatures of Homogenization and $H_2O$ Concentrations," Chem. Geol. **183**, 87–98 (2002).
22. W. F. McDonough, S. S. Sun, A. E. Ringwood, et al., "K, Rb and Cs in the Earth and Moon and the Evolution of the Mantle of the Earth," Geochim. Cosmochim. Acta **56**, 1001–1012 (1992).
23. P. Michael, "Regionally Distinctive Sources of Depleted MORB: Evidence from Trace Elements and $H_2O$," Earth Planet. Sci. Lett. **131**, 301–320 (1995).
24. V. B. Naumov, V. I. Kovalenko, V. V. Yarmolyuk, and V. A. Dorofeeva, "Volatile Components ($H_2O$, Cl, F, S, and $CO_2$) in Magmatic Melts of Various Geodynamic Environments," Geokhimiya, No. 5, 555–564 (2000) [Geochem. Int. **38**, 500–509 (2000)].
25. V. B. Naumov, V. I. Kovalenko, V. V. Yarmolyuk, and V. A. Dorofeeva, "Average Concentrations of Major, Volatile, and Trace Elements in Magmas of Various Geodynamic Settings," Geokhimiya, No. 10, 1113–1124 (2004) [Geochem. Int. **42**, 977–987 (2004)].
26. H. Palme and H. St. C. O'Neill, "Cosmochemical Estimates of Mantle Composition," in *Treatise on Geochemistry* (Elsevier, Amsterdam, 2003), Vol. 2, pp. 1–38.
27. P. Philippot, P. Agrinier, and M. Scambelluri, "Chlorine Cycling during Subduction of Altered Oceanic Crust," Earth Planet. Sci. Lett. **161**, 33–44 (1998).
28. Z. Quin, F. Lu, and A. T. Anderson, "Diffusive Re-Equilibration of Melt and Fluid Inclusions," Am. Mineral. **77**, 565–576 (1992).
29. A. B. Ronov, A. A. Yaroshevskii, and A. A. Migdisov, *Chemical Structure of the Earth's Crust and Geochemical Balance of Major Elements* (Nauka, Moscow, 1990) [in Russian].
30. R. L. Rudnick and S. Gao, "Composition of the Continental Crust," in *Treatise on Geochemistry* (Elsevier, Amsterdam, 2003), Vol. 3, pp. 1–64.
31. I. D. Ryabchikov, *Thermodynamic Analysis of the Behavior of Minor Elements during Silicate Melt Crystallization* (Nauka, Moscow, 1965) [in Russian].
32. A. E. Saal, E. H. Hauri, C. H. Langmuir, and M. R. Perfit, "Vapour Undersaturation in Primitive Mid-Ocean-Ridge Basalt and the Volatile Content of Earth's Upper Mantle," Nature **419**, 451–455 (2002).
33. V. J. M. Salters and A. Stracke, "The Composition of the Depleted Mantle," Geochem. Geophys. Geosyst. **5** (5), 1–27 (2004).
34. J.-G. Schilling, M. B. Bergeron, and R. Evans, "Halogens in the Mantle beneath the North Atlantic," Philos. Trans. R. Soc. London **A297**, 147–178 (1980).
35. G. Sen, A. Macfarlane, and N. Srimal, "Significance of Rare Hydrous Alkaline Melts in Hawaiian Xenoliths," Contrib. Mineral. Petrol. **122**, 415–427 (1996).
36. D. M. Shaw, "Trace Element Fractionation during Anatexis," Geochim. Cosmochim. Acta **34**, 237–243 (1970).
37. K. Simons, J. Dixon, J.-G. Schilling, et al., "Volatiles in Basaltic Glasses from the Easter–Salas y Gomez Seamount Chain and Easter Microplate: Implication for Geochemical Cycling of Volatile Elements," Geochem. Geophys. Geosyst. **3** (7), 1–29 (2002).
38. A. V. Sobolev and L. V. Danyushevsky, "Petrology and Geochemistry of Boninites from the North Termination of the Tonga Trench: Constraints on the Generation Conditions of Primary High Ca Boninite Magmas," J. Petrol. **35**, 1183–1211 (1994).
39. A. V. Sobolev, A. W. Hofmann, S. V. Sobolev, and I. K. Nikogosian, "An Olivine-Free Mantle Source of Hawaiian Shield Basalts," Nature **434**, 590–597 (2005).
40. R. K. Workman and S. R. Hart, "Major and Trace Element Composition of the Depleted MORB Mantle (DMM)," Earth Planet. Sci. Lett. **231**, 53–72 (2005).